

**CIRCULATION COPY**  
**SUBJECT TO RECALL**  
**IN TWO WEEKS**

**UCRL-92324**  
**PREPRINT**

**Climatic Response to Large Summertime  
Injections of Smoke into the Atmosphere:  
Changes in Precipitation and the  
Hadley Circulation**

**Steven J. Ghan  
Michael C. MacCracken  
John J. Walton**

**This paper was prepared for submittal to  
International Association for Meteorology  
and Atmospheric Physics  
Honolulu, Hawaii  
August 5-16, 1985**

**August, 1985**

**Lawrence  
Livermore  
National  
Laboratory**

**This is a preprint of a paper intended for publication in a journal or proceedings. Since changes may be made before publication, this preprint is made available with the understanding that it will not be cited or reproduced without the permission of the author.**

#### DISCLAIMER

This document was prepared as an account of work sponsored by an agency of the United States Government. Neither the United States Government nor the University of California nor any of their employees, makes any warranty, express or implied, or assumes any legal liability or responsibility for the accuracy, completeness, or usefulness of any information, apparatus, product, or process disclosed, or represents that its use would not infringe privately owned rights. Reference herein to any specific commercial product, process, or service by trade name, trademark, manufacturer, or otherwise, does not necessarily constitute or imply its endorsement, recommendation, or favoring by the United States Government or the University of California. The views and opinions of authors expressed herein do not necessarily state or reflect those of the United States Government or the University of California, and shall not be used for advertising or product endorsement purposes.

# **Climatic Response to Large Summertime Injections of Smoke into the Atmosphere: Changes in Precipitation and the Hadley Circulation**

**Steven J. Ghan, Michael C. MacCracken and John J. Walton**  
**Atmospheric and Geophysical Sciences Division**  
**Lawrence Livermore National Laboratory**  
**University of California**

**August 1985**

## **ABSTRACT**

An atmospheric general circulation model (AGCM) has been initialized with a 150 Tg summertime injection of smoke from post-war fires over Europe, Asia and North America. The smoke is subject to large-scale and convective transport, dry deposition, coagulation and precipitation scavenging. The Hadley circulation is shown to respond in three stages. In the first stage, which lasts about one week depending on initial conditions, the Hadley circulation doubles in intensity. As the smoke spreads across the equator, and as the troposphere becomes more stable, the Hadley cell then weakens until it becomes actually weaker than in the control climate. In the final stage, as the smoke is removed, the Hadley cell gradually returns towards the control.

Surface precipitation generally decreases as a result of the smoke. By the fourth week following the injection, zonal-mean surface precipitation in the tropics and summer hemisphere midlatitudes are about half of those in the control climate. The decrease is most notable over land, ocean precipitation being reduced only in the tropics. Penetrating convective precipitation is greatly reduced at all latitudes; large-scale precipitation is enhanced, becoming the dominant mode of precipitation in the simulation. Precipitation over land is shown to decrease significantly for smoke loadings insufficient to produce long-term land surface cooling. It is suggested that regions of surface warming following the smoke injection result from surface drying reducing the efficiency of evapotranspiration.

Precipitation scavenging is shown to be the dominant removal process for particles larger than one micron in diameter. As a result, the lifetime of large particles increases several-fold due to the reduction in precipitation and the "self-lofting" of the smoke. For particles smaller than one micron in diameter, precipitation scavenging is found to be a much less efficient removal mechanism than both coagulation, which is important during the first week following the injection, and dry deposition at later times. The inefficiency of precipitation scavenging of small particles is due to the small value of the assumed scavenging coefficient, which is a factor of 40 smaller than that used for large particles. Empirical evidence is presented in support of the use of such a small scavenging coefficient.

## INTRODUCTION

The simulation of the climatic effects of a nuclear war has progressed rapidly in recent years. Within two years the initial one-dimensional study of Turco et al. (1983) has been followed by two-dimensional (MacCracken, 1983) and three-dimensional simulations with fixed distributions of smoke (Aleksandrov and Stenchikov, 1983; Covey et al., 1984; Cess et al., 1985), and more recently by two-dimensional (Haberle et al., 1985) and three-dimensional (MacCracken and Walton, 1984; Malone et al. 1985; Thompson, 1985) simulations with smoke transported and removed by the atmospheric circulation with which it interacts. The principal focus of these studies has been surface air temperature, understandably, since it is the primary climate variable. However, numerous aspects of the simulations have not been examined. In particular, the field of precipitation has received relatively little attention. Although the reasons for this undoubtedly lie in a lack of confidence in the simulated precipitation rates, the importance of precipitation both as a climate variable and as a means of smoke removal prompts the conclusion that the field of simulated precipitation merits further investigation. It is the purpose of this paper to consider changes in the field of precipitation in general circulation model experiments involving moving smoke. Related aspects of the simulation will also be examined.

Results to be discussed will come from primarily one experiment, in which 150 Tg of smoke are instantaneously injected over the North American and Eurasian continents in July. The month of July was chosen because the response to a Northern Hemisphere injection is greatest in July. We shall restrict our discussion to the evolution of the Hadley circulation, changes in the type and distribution of precipitation, and the budgets of globally integrated smoke mass. In particular, we will attempt to demonstrate that the Hadley circulation responds to the smoke loading in three stages, that convective precipitation is virtually eliminated, and that stratiform precipitation replaces convective precipitation and occurs only over the oceans at low levels. This latter result will be shown to hold even for smoke loadings sufficiently small as to yield long-term surface warming. (Long-term is

defined as periods comparable to the radiative response time for the troposphere, which is about thirty days as opposed to the land surface response time of less than one day). We will also show that precipitation scavenging is the principle removal mechanism for the large particles, but not for the submicron particles. Because this result depends on the specified scavenging coefficients, we will present empirical evidence supporting the use of relatively small scavenging coefficients for submicron particles.

## MODELS AND SMOKE

The experiments involve perpetual July conditions simulated by the Oregon State University two-level tropospheric general circulation model (Schlesinger and Gates, 1980; Ghan et al., 1982), modified by the incorporation of a delta-Eddington formulation for solar radiation (Cess et al., 1985), and coupled to a Lagrangian trace species transport model known as GRANTOUR (Walton and MacCracken, 1984).

GRANTOUR employs a sampler parcel technique, wherein parcels of air carrying masses of various particle types are advected by the simulated atmospheric circulation. This method for treating advection is extremely accurate and non-diffusive, and ensures that particle mass is conserved and that negative particle concentrations do not arise. Two types of particles are carried in the parcels, one representing particles sub-micron in diameter, the other representing particles larger than one micron. The extinction cross section is assumed to be  $6.7 \text{ m}^2/\text{g}$  for the small particles and  $2.8 \text{ m}^2/\text{g}$  for the large particles. A single-scatter albedo of 0.5 is assumed for both particle types. These particles are subject to dry deposition and coagulation as well as precipitation scavenging and large-scale and convective transport. The deposition velocities are 1 cm/s and 0.2 cm/s for the large and small particle types, respectively, with the removal due to dry deposition applied to air parcels with centroids within 4 km of the surface at rates assumed to decrease linearly to zero at 4 km. Coagulation is parameterized assuming Brownian diffusion based on calculations by Penner (1984, personal communication), and is given by

$$\frac{dc_2}{dt} = -2.0 \times 10^6 (c_1 + c_2) c_2 \quad (1)$$

where  $c_1$  and  $c_2$  are the mass concentrations of the large and small particles, respectively. Precipitation scavenging is in direct proportion to the precipitation rate, with the scavenging coefficients taken from Dana and Hales (1976). For large-scale (frontal) precipitation the scavenging coefficients are  $8 \text{ cm}^{-1}$  and  $0.2 \text{ cm}^{-1}$  for the large and small particles, respectively, while for convective precipitation they are  $3 \text{ cm}^{-1}$  and  $0.07 \text{ cm}^{-1}$ , respectively.

Patchiness of precipitation systems is also accounted for. Because precipitation scavenging is exponential, less smoke will be removed if precipitation occurs in isolated convective towers than if it occurs over a broad region. For our purposes we have assumed that convective precipitation covers 20% of a model grid box, while large-scale precipitation covers 75% of the area. Note that the smaller scavenging coefficients given above for convective precipitation account only for the different size distribution of convective raindrops, and do not account for the greater patchiness associated with convective precipitation.

The initial distribution of the smoke loading as represented by the extinction optical depth is illustrated in Fig. 1. Equal masses of smoke have been injected from each of 5 large areas, two covering North America and three in Eurasia, distributed initially in the vertical with a constant smoke mixing ratio between the surface and 200 mb. The total mass of 150 Tg is composed of 90 Tg of particles smaller than and 60 Tg of particles larger than one micron. Optical depths exceeding 50 are found over both continents. Note that the smoke is initially isolated from the region of strong convection associated with the southeast Asian monsoon. Thus, it takes several days for the smoke to reach the limb of the Hadley circulation.

### THE HADLEY CIRCULATION

Fig. 2 depicts a measure of the Hadley circulation as a function of time. The quantity contoured is the northward flux of mass between 200 mb (the model top) and 600 mb, integrated in longitude and plotted as a function of latitude and time. One common measure

of the strength of the Hadley circulation is the mean meridional mass flux streamfunction, which is usually plotted as a function of latitude and height; Fig. 2 shows the value of that stream function at 600 mb (the only level for which it is defined in the two-level AGCM), plotted as a function of latitude and time. Note that the values largest in magnitude are negative, representing southward upper tropospheric flow associated with the southern branch of the Hadley circulation (the northern branch has all but disappeared, but is very weak in the control, as observed at this time of year). Note also that the control mass flux exhibits considerable variability, both over the diurnal cycle (which has been filtered out here) and for the synoptic time scale, where values for the control Hadley circulation range between roughly 200 and  $300 \times 10^9$  kg/s. The observed Hadley cell strength in July is thought to be about 200, so the control case Hadley cell is a bit too strong.

In the presence of smoke, we find a rather considerable modification to the Hadley circulation. This is nothing new in itself; Covey et al., (1984) found a similar result for the NCAR model with a fixed distribution of smoke. What is interesting here is the structure of the change. As expected, the Hadley cell accelerates as the smoke approaches the limb of the circulation, with peak values exceeding 500, or about double the intensity of the control circulation. However, after about one week the Hadley circulation begins to weaken. This happens for two reasons. First, the obvious reason is that the smoke has spread across the equator, thereby reducing the heating gradient associated with the smoke. This is to be expected, since as noted by Covey et al., it is the smoke-induced heating gradient that initially accelerates the Hadley circulation. There is another reason for the weakening, however. As noted by others, the static stability of the troposphere is considerably enhanced by solar heating due to the smoke. The Hadley circulation can then transport heat laterally much more efficiently. Thus, for the same heating gradient, a weaker Hadley cell will transport the same amount of heat. If the smoke spreads sufficiently so that the heating gradient is comparable to that of the control atmosphere, a Hadley cell actually weaker than the control is possible. This is the case for the smoke loading

considered here. After three weeks following the smoke injection, the Hadley cell has weakened to about  $200 \times 10^9$  kg/s. Although not substantially weaker than the control Hadley circulation, evidence from experiments with larger injections or with no smoke removal, supports the conclusion that tropospheric stabilization by solar absorption by the smoke weakens the Hadley circulation. The time scale for such a weakening is the radiative time scale for the troposphere, about one month. By this time, however, the Hadley cell has already completed the task of transporting the smoke across the equator. Assuming the Hadley cell returns to full strength as the smoke is removed from the atmosphere, we have then three stages in the evolution of the Hadley cell for a large summertime injection: First, strengthening to about double the control intensity, then weakening to a level somewhat below that of the control, and finally a gradual return to the control circulation. The time scale for the first phase is determined by the time it takes the smoke to reach the limb of the Hadley circulation. The time scale for the second stage is governed by the radiative time scale for the troposphere. The third phase depends on the time scale of smoke removal from the atmosphere.

### PRECIPITATION

We will now consider the precipitation changes simulated by the AGCM. There are significant modifications to precipitation rates in the presence of smoke loadings, changes that occur for loadings smaller than required for significant long-term reductions in surface temperature. These changes are generally negative, i.e., precipitation is reduced. To satisfy concerns with respect to the statistical significance of the results to follow, Fig. 3 shows the long-term mean and the standard deviation of ten-day means of the control precipitation averaged in longitude. The standard deviation is presented in order to establish the variability of the ten-day means to be presented in subsequent figures. According to Fig. 3, the variability of ten-day mean precipitation is nearly everywhere less than one half mm/day. Because this level of variability is typical of that found for the other types of mean precipitation to be discussed, no other standard deviations will be presented.



All general circulation models distinguish between large-scale and convective precipitation. Fig. 4 illustrates these two forms of precipitation as simulated by the OSU AGCM. Large-scale precipitation occurs when relative humidity exceeds a prescribed saturation value; convective precipitation depends on vertical stability and, for some general circulation models, also on the occurrence of saturation.

Because of the differing dependence of these two forms of precipitation, they are expected to respond in different ways to modifications to the atmospheric structure. In particular, the outstanding feature of the response to large injections of smoke is the stabilization of the troposphere. As a result, convective precipitation decreases in response to smoke loadings more so than large-scale precipitation. Since, as is evident from Fig. 4, the control convective precipitation dominates large-scale precipitation at all latitudes except in the polar regions and the winter hemisphere mid-latitudes, one might expect the total precipitation to be sensitive to smoke loadings in the tropics, subtropics and summer hemisphere mid-latitudes.

Fig. 5 shows the total precipitation rate plotted again for the 30-day control and also for the 150 Tg summertime injection averaged over days 1- 10, 11-20 and 21-30 after injection. The first feature of interest is the initial increase in tropical precipitation. This is consistent with the early acceleration of the Hadley circulation noted previously. At later times however, precipitation in the tropics is drastically reduced. This is associated with the stabilization of the troposphere as the upper troposphere warms because of solar heating. This suggests a tropospheric radiative time scale for the response.

In northern mid-latitudes, precipitation decreases even for early times, indicative of a process with a time scale much shorter than the radiative time scale for the atmosphere. That process is surface cooling over land, which can be quite rapid (i.e., the diurnal cycle). We shall provide more evidence for this assertion shortly. Convective precipitation is illustrated in Fig. 6 for the 30-day control and for the 150 Tg injection 1-10, 11-20 and 21-30 days after the smoke injection. Convective precipitation has been virtually eliminated

from the simulation. There is a caveat, however. The convective precipitation represented by the two-level AGCM is penetrative, i.e., it is assumed to extend through the entire depth of the troposphere. Shallow convection is assumed to modify the boundary layer but produces no precipitation. In the real world, or in a GCM with finer vertical resolution, one may find shallow forms of precipitating convection, especially off the east coasts of the major continents.

Fig. 7 shows the large-scale precipitation simulated for the July control simulation and for the three 10-day periods following the injection. Large-scale precipitation is enhanced by the presense of the smoke. Note that this is not due to the low-level cooling associated with the smoke. In fact, the lowest atmospheric layer cools very little (the surface cools of course, but condensation is only allowed from the atmospheric layers). Large-scale precipitation is enhanced because convective precipitation has been suppressed. Whereas in the control atmosphere moist convection removes water vapor before large-scale supersaturation occurs, in the presence of the smoke moistening due to advection and surface evaporation continues until supersaturation is achieved. This suggests that large-scale and convective precipitation are complementary. Indeed, in general circulation experiments conducted by Miyakoda and Sirutis (1984) in which the moist convective adjustment was turned off, estimated precipitation was surprisingly similar to experiments with parameterized moist convection.

Fig. 8 shows the total precipitation again, but this time for ocean areas only. In this case the only significant decrease is in the tropics. In mid-latitudes, the perturbed precipitation rate is close to that in the control, in spite of a nearly complete switch from convective to large-scale precipitation. In the tropics the response is quite slow, partly because the smoke has not been injected there, but also because radiative heating in the upper troposphere is the only way to reduce convective precipitation over the ocean. Interestingly, large-scale precipitation is unable to fully compensate for the decrease in convective precipitation in the tropics. This is probably related to the weakening of the Hadley circulation.

Just as the response of surface air temperature for land is very different than for ocean, the response of precipitation for land is also very different. Fig. 9 shows the total precipitation again, but this time for land only. Here the response is greater, with significant decreases in northern mid-latitudes as well as in the tropics. Note that the response in mid-latitudes is particularly rapid. This is, of course, because the smoke was injected there. Since experiments with uniform smoke indicate an even more rapid response, we conclude that the time scale for the response is determined by the time it takes the smoke to spread. That is, once the smoke is present, land precipitation decreases rapidly. This is consistent with the rapid response of surface land temperature.

One question which comes to mind at this point is, why doesn't large-scale precipitation increase to compensate for the reduction in convective precipitation, as it does over the ocean? The answer must lie in moisture availability. Surface evaporation over land is suppressed as a result of the surface cooling. Also, as noted by Covey et al., (1985), the atmosphere responds to a uniform distribution of smoke with what may be considered a continental-scale land breeze, with subsidence at low levels over land. Such a circulation will not transport moisture to land very efficiently. Thus, moistening due to both advection and surface evaporation is reduced over land.

The increase in precipitation at  $30^{\circ}\text{N}$  is probably an example of a model deficiency, for physical intuition argues strongly against it. A latitude-longitude map of precipitation (not shown) indicates that the increase is due to an enhancement of the southeast Asian monsoon. The reason for this lies in the crude vertical resolution of the two-layer model. A large portion of the smoke remains in southeast Asia in the upper troposphere. The associated solar heating is driving upward-vertical motion. This in itself is not a problem. What is a problem is that, since the vertical velocity is carried at only one level in the two-layer model, the upward motion implies adiabatic cooling in both the model's lower and upper layers. This cooling and the associated convergence of moisture result in large-scale condensation within the lower layer. In the real atmosphere, or in a model with finer

vertical resolution, the upward vertical motion would probably be confined to the layers with radiative heating. This kind of response is what was found in the NCAR 9-level model by Covey et al., (1985).

A recent paper by Cess et al. (1985) demonstrates that, for distributions of smoke such that significant solar absorption occurs in the lower troposphere, long-term surface warming follows early time surface cooling. The long-term surface warming is shown to result from enhancement of the downward flux of infrared radiation due to warming and moistening of the lower troposphere. The short-term cooling is of course due to the reduction in solar radiation at the surface, which is only partially compensated by a reduction in surface convection. Fig. 10 shows the change in surface air temperature over land for days 1-10, 11-20 and 21-30 following a smaller 50 Tg summertime injection. This 50 Tg injection is small enough to allow significant amounts of sunlight to penetrate to the lower troposphere where it can be absorbed. We should then find a response similar to that found by Cess et al. with a 1- dimensional radiative-convective model. According to Fig. 10, the early time local cooling of the land surface by about 10 degrees is followed by a long term surface warming of nearly 5 degrees.

One of the points of the paper by Cess et al. (1985) is that convection is eliminated for amounts of smoke smaller than are required to produce a long-term surface cooling. That is, surface cooling results only when the surface and troposphere are convectively decoupled. Since moist convection is the primary form of precipitation in the tropics and summer hemisphere mid-latitudes, significant decreases in land precipitation are expected for smoke loadings too small to produce a long-term surface cooling.

Fig. 11 shows land precipitation for the control again and for days 1-10, 11-20, and 21-30 following the 50 Tg smoke injection. The decrease in land precipitation for the 50 Tg injection is comparable to that for the 150 Tg projection. Tropical precipitation has not been reduced as much as for 150 Tg, but the nonphysical enhancement of the southeast Asian monsoon is absent. On the basis of this experiment, we conclude that substantial

reductions in land precipitation are possible for smoke loadings that yield long-term surface warming and only modest early-time surface cooling.

Precipitation is reduced at other levels of the atmosphere as well. In Fig. 12 the precipitation at the mid-level of the model, about 600 mb, is plotted for the control and for days 1-10, 11-20 and 21-30 following the 150 Tg injection. This is of interest because of the importance of precipitation scavenging in the removal of the smoke. Upper-tropospheric precipitation is greatly reduced under the presence of smoke. This is no great surprise, of course, since the smoke is heating the air at that level.

### GROUND HYDROLOGY

We shall now focus briefly on one feedback that has not been considered in the context of "nuclear winter" studies, but which is worth mentioning. It is well known that, in equilibrium, a dry surface will be warmer than a wet surface for a given insolation. This is because a wet surface can cool through evaporation as well as through sensible heat transfer and emission of longwave radiation to the atmosphere. Since we have found a significant decrease in precipitation over land as a result of tropospheric smoke loading, one should expect to find drier land surfaces as well. And since the OSU AGCM simulates a surface hydrology, we can examine this feedback.

The ground wetness simulated by the model for perpetual July is plotted in Fig. 13. Ground wetness is defined to be the ratio of the surface water content to the field capacity, which is assumed to be  $15g/cm^2$ . The feature of interest is the band of moist ground across equatorial Africa. This is associated with the simulated rainy season in Africa. The ground wetness there is about one half, which is the value above which evapotranspiration is assumed to function at maximum efficiency.

Fig. 14 shows the ground wetness averaged for days 21-30 following the 150 Tg injection. Note now that the ground moisture formerly in equatorial Africa has disappeared, with values for the ground wetness now less than one tenth. Note also the spurious moistening in southeast Asia associated with the enhanced monsoon.

As a result of the surface drying, the surface air temperature has risen across equatorial Africa. Fig. 15 shows the difference in surface air temperature between the 150 Tg and control cases for days 21-30 following the injection. The warming exceeds ten degrees. Because the region of surface warming corresponds well with the region of surface drying, it is unlikely that the warming is due only to enhanced downward infrared flux at the surface.

### SMOKE PARTICLE LIFETIMES

As stated previously, two sizes of smoke particles are accounted for. Fig. 16 illustrates the total mass of large particles plotted as a function of time for the 150 Tg injection and for the control atmosphere, i.e., one in which the interaction of the smoke with radiation has been turned off. As expected, much more smoke remains when the radiative interaction is included. This is both because the smoke tends to be lofted into the upper troposphere, above precipitation, and because precipitation has been reduced. As a result, the lifetime (Fig. 17) for the large particles has been increased several-fold, from 5-10 days to about 50 days.

Fig. 18 shows the time history of the total mass of small particles. Here we find very little difference in the two time histories. This suggests that precipitation scavenging is not an important removal process for the small particles as simulated here. The corresponding lifetime (Fig. 19) indicates no difference in the lifetimes at early times, but then a gradual divergence at later times.

The total mass (Fig. 20) of both sizes of smoke particles exhibits only a modest difference between the control and interactive cases. The total smoke lifetime (Fig. 21), though some 50% longer, for the interactive case, is not the several times longer as might have been expected on the basis of the initial studies by Malone et al. (1985).

We shall now consider the reasons for this. Although one can justifiably argue that the presence of a model lid at the tropopause prevents the particle lifetimes from increasing further, there are additional reasons. Fig. 22 shows the large particle lifetime for a control

(non-interactive) simulation with the particles subject to coagulation, scavenging and dry deposition individually. This illustrates the relative importance of the different processes. The coagulation lifetime for the large particles is of course ill-defined since coagulation increases the total large particle mass. The lifetime associated with precipitation scavenging is much shorter than that for dry deposition, indicating that scavenging is a much more efficient mechanism for removal of large particles than is dry deposition. (This, of course, depends on the vertical distribution of the particles, which changes in time). Note that the scavenging lifetime is 5–10 days, while the dry deposition removal time is 10–30 days.

Fig. 23 corresponds to Fig. 22 but applies to the small particles. During the first week following the smoke injection, coagulation of the small particles is seen to be the most efficient removal mechanism. As the particles disperse, the coagulation rate decreases until after several weeks dry deposition becomes the principal removal process. At no time is precipitation scavenging a significant factor in the removal of the small particles. Instead, small particles are removed either directly through dry deposition or indirectly through coagulation and then later scavenged as large particles.

We shall now attempt to assess validity of the parameterization of the scavenging mechanism that is used. The scavenging time for the large particles is 5–10 days, compared with the approximately 150 day scavenging time for the small particles. This is a ratio of 15–30 in the scavenging rates for the two particle species.

There is much dispute as to the proper scavenging coefficients for the small particles. We have used values of 0.2 and  $0.07 \text{ cm}^{-1}$  for scavenging by large-scale and convective precipitation, respectively. These values are a factor of some forty smaller than the corresponding values of 8 and  $3 \text{ cm}^{-1}$  for large particles. But these are theoretical values, taken from Dana and Hales (1976). Their estimate neglects certain processes, such as nucleation. Some would argue that the scavenging coefficients for the small particles should be much larger.

Empirical evidence can be used to estimate upper bounds for the small-particle scavenging coefficient. Dr. Anthony Clark of the University of Washington has made measurements of what he calls the washout ratio, which is the ratio of the mixing ratio of soot in snow to the mixing ratio of aerosols in arctic air. Since aerosols in the arctic are long-lived sub micron aerosols similar to small urban soot aerosols, the aerosols might be expected to have similar scavenging coefficients. An upper bound on the scavenging coefficient for aerosols in the arctic can be found by assuming that all soot is deposited on the snow by precipitation scavenging. To the extent that this is not true, we will overestimate the scavenging coefficient. The washout ratio can then be expressed

$$w \geq \frac{\rho_a}{\rho_w} S h \quad (2)$$

where  $\rho_w$ ,  $\rho_a$  and  $\rho_s$  are the densities of water, air and aerosol, respectively;  $P$  is the precipitation rate;  $S$  the aerosol scavenging coefficient; and

$$\begin{aligned} h &\equiv \int_0^\infty \rho_s S P dz / (\bar{\rho}_s S P_o) \\ &\simeq \int_0^\infty \rho_s P dz / (\bar{\rho}_s P_o) \end{aligned} \quad (3)$$

is a measure of the characteristic vertical scale of the aerosol and of precipitation when scavenging occurs. The upper bound for the scavenging coefficient is then given by

$$S \leq \frac{\rho_w}{\rho_a} \frac{w}{h} \quad (4)$$

Observations by Rosen and Hansen (1984) indicate considerable variability in the vertical distribution of arctic aerosols, but vertical profiles for precipitation-free conditions suggest that the aerosols are distributed through a depth of at least one kilometer. Assuming that the precipitation also occurs through a depth of at least one kilometer, then Clark's (personal communication) observed washout ratio of 150 yields a scavenging coefficient no greater than  $1.5 \text{ cm}^{-1}$ . Although this is considerably larger than the value of 0.2 that we have used in our experiments, it is also substantially smaller than the coefficient



used for the large particles. If one wishes to account for dry deposition as well, the upper bound could easily be cut in half to  $0.75 \text{ cm}^{-1}$ . This is a factor of ten smaller than the coefficient used for large particles.

## SUMMARY

In conclusion, we have presented evidence for a three-stage evolution of the Hadley circulation under a large summertime loading of highly absorbing smoke. The Hadley circulation first intensifies when the smoke first reaches its edge, then decays as the smoke is spread to the Southern Hemisphere by the Hadley circulation and as the troposphere is stabilized, and then finally returns to normal strength as the smoke is removed from the atmosphere. We have shown that precipitation is greatly reduced over land, even for more modest injections of smoke that produce moderate surface cooling and long term surface warming. Over the oceans, there is little change in precipitation in mid-latitudes, but a significant reduction in the tropics. Convective precipitation is replaced by stratiform precipitation. This does not occur over land because of reduced surface evaporation and ocean-to-land moisture transport. Precipitation from the upper troposphere is greatly reduced.

Surface drying associated with reduced precipitation over land has been identified as a mechanism for surface warming. We have also presented evidence in support of the use of the small theoretical scavenging coefficients for submicron particles.

There are caveats of course, all of which are related to the restricted vertical resolution of the model employed. We wish to emphasize first that the OSU two-layer model has proven to be very valuable as an economical and credible tool in the investigation of such issues as the transient response to increasing concentrations of  $\text{CO}_2$  in the atmosphere. This is because, as discussed by Potter and Cess (1984), the surface and troposphere respond as a highly coupled system for the present climate. For the conditions of a nuclear winter, however, convection is suppressed. The surface and troposphere no longer respond as a unit. The vertical structure of the heating and the dynamical response must be

adequately resolved. We have presented evidence of an apparently spurious enhancement of the southeast Asian monsoon because of the two-layer model's crude vertical resolution. We also know that transport of the smoke into the stratosphere could be an important factor in extending the smoke lifetime. This would also allow long-term surface cooling for moderate smoke injections, since the stratosphere is already convectively decoupled from the troposphere. Thus, although certain issues can be economically explored with the two-layer model, models with finer vertical resolution must be employed for the more definitive answers.

## ACKNOWLEDGEMENTS

The authors wish to express a hearty thanks to A. R. Licuanan for his diligence in performing the model integrations. This work was performed under the auspices of the U.S. Department of Energy by the Lawrence Livermore National Laboratory under contract No. W-7405-Eng-48.

## REFERENCES

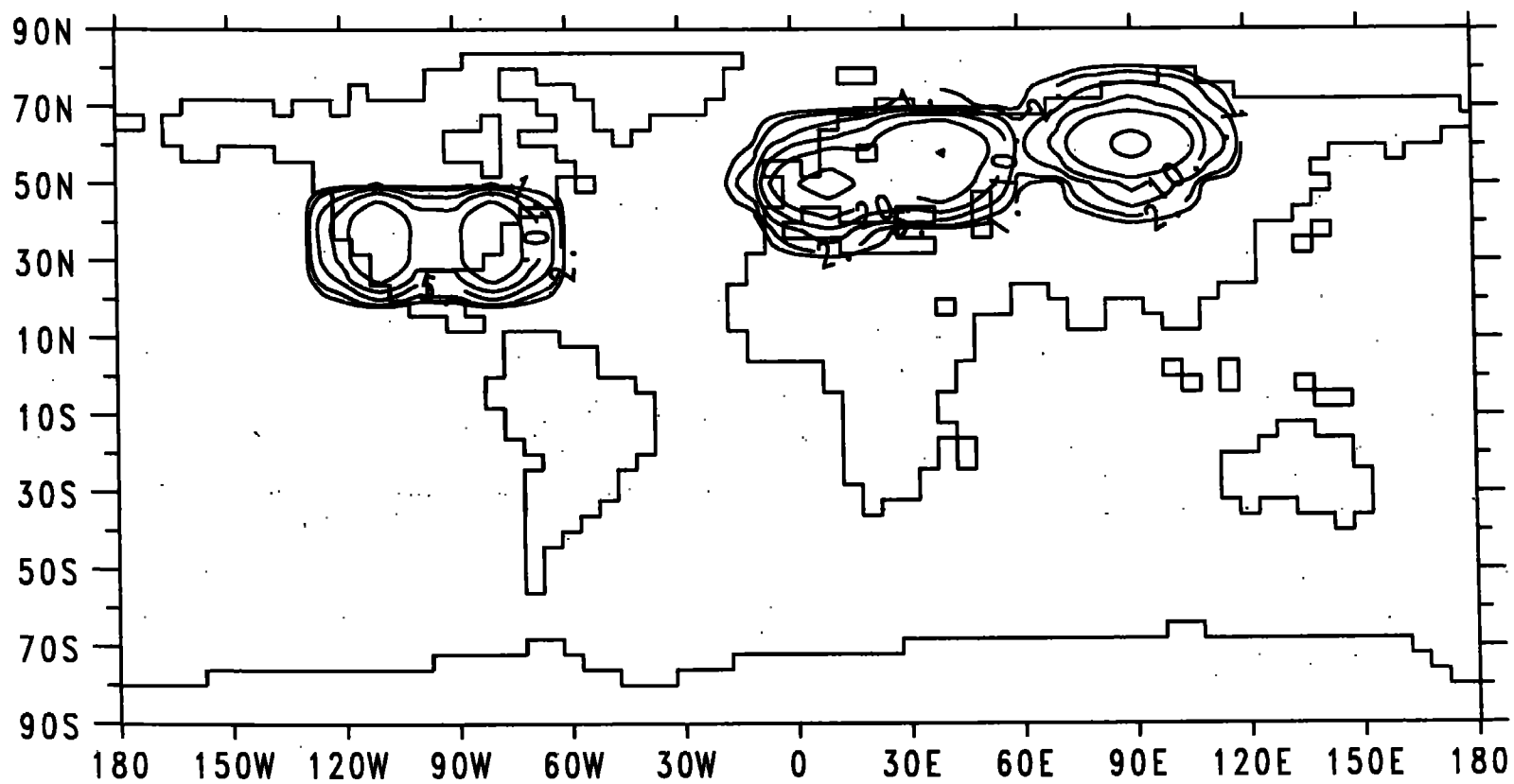
- Aleksandrov, V. and Stenchikov, G. L. (1983): On the modelling of the climatic consequences of the nuclear war. *The Proceedings on Applied Mathematics (1983)*, The Computing Centre of the USSR Academy of Sciences, Moscow.
- Cess, R. D., G. L. Potter, S. J. Ghan and W. L. Gates, 1985: The climatic effects of large injections of atmospheric smoke and dust: A study of climatic mechanisms with one-and three-dimensional climate models. *J. Geophys. Res.*, accepted for publication.
- Covey, C., S. H. Schneider and S. L. Thompson, 1984: Global atmospheric effects of massive smoke injections from a nuclear war: Results from general circulation model simulations. *Nature*, 308, 21-25.
- Covey, C., S. L. Thompson and S.H. Schneider, 1985: "Nuclear winter": A diagnosis of atmospheric general circulation model simulations. *J. Geophys. Res.*, 90, 5615-5628.

- Ghan, S. J., J. W. Lingaas, M. E. Schlesinger, R. L. Mobley and W. L. Gates, 1982: A documentation of the OSU two-level atmospheric general circulation model. *Climatic Research Institute Report No. 35*, Oregon State University, Corvallis, OR 97331, 395pp
- Haberle, R. M., T. P. Ackerman, O. B. Toon and J. L. Hollingsworth, 1985: Global transport of atmospheric smoke following a major nuclear exchange. *Geophys. Res. Lett.*, submitted
- MacCracken, M. C., 1983: Nuclear war: preliminary estimates of the climatic effects of a nuclear exchange. Lawrence Livermore National Laboratory Report, UCRL-89770, October, 1983.
- MacCracken, M.C., and J.J. Walton, 1984: The effects of interactive transport and scavenging on the calculated temperature change resulting from large amounts of smoke. Lawrence Livermore National Laboratory Report, UCRL-91446, December, 1984.
- Malone, R.C., L.H. Auer, G.A. Glatzmaier, M.C. Wood and O.B. Toon, 1985: Nuclear winter: Three dimensional simulations including interactive transport, scavenging and solar heating of smoke. *J. Geophys. Res.*, submitted.
- Miyakoda, K., and J. Sirutis, 1984: Impact of subgrid-scale parameterization on monthly forecasts. Geophysical Fluid Dynamics Laboratory/NOAA, Princeton, New Jersey.
- Potter, G.L., and R.D. Cess, 1984: Background tropospheric aerosols: Incorporation within a statistical-dynamical climate model. *J. Geophys. Res.*, 89, 9521-9526.
- Rosen, H., and A.D.A. Hansen, 1984: Role of combustion-generated carbon particles in the absorption of solar radiation in the arctic haze. *Geophys. Res. Lett.*, 11, 461-464.
- Schlesinger, M.E., and W.L. Gates, 1980: The January and July performance of the OSU two-level atmospheric general circulation model. *J. Atmos. Sci.*, 37, 1914-1943.
- Thompson, S. L. 1985: Global interactive transport simulations of nuclear war smoke. *Nature*, In press.
- Turco, R.P., O.B. Toon, T.P. Ackerman, J.B. Pollack and C. Sagan, 1983: Nuclear winter: Global consequences of multiple nuclear explosions. *Science*, 222, 1283-1292.

**Walton, J.J., and M.C. MacCracken, 1984: Preliminary report on the global transport model GRANTOUR. Lawrence Livermore National Laboratory Report, UCID-19985, January, 1984**

Figure 1. Initial distribution of smoke extinction optical depth for a 150 Tg injection of smoke.

## SMOKE OPTICAL DEPTH INITIAL DISTRIBUTION



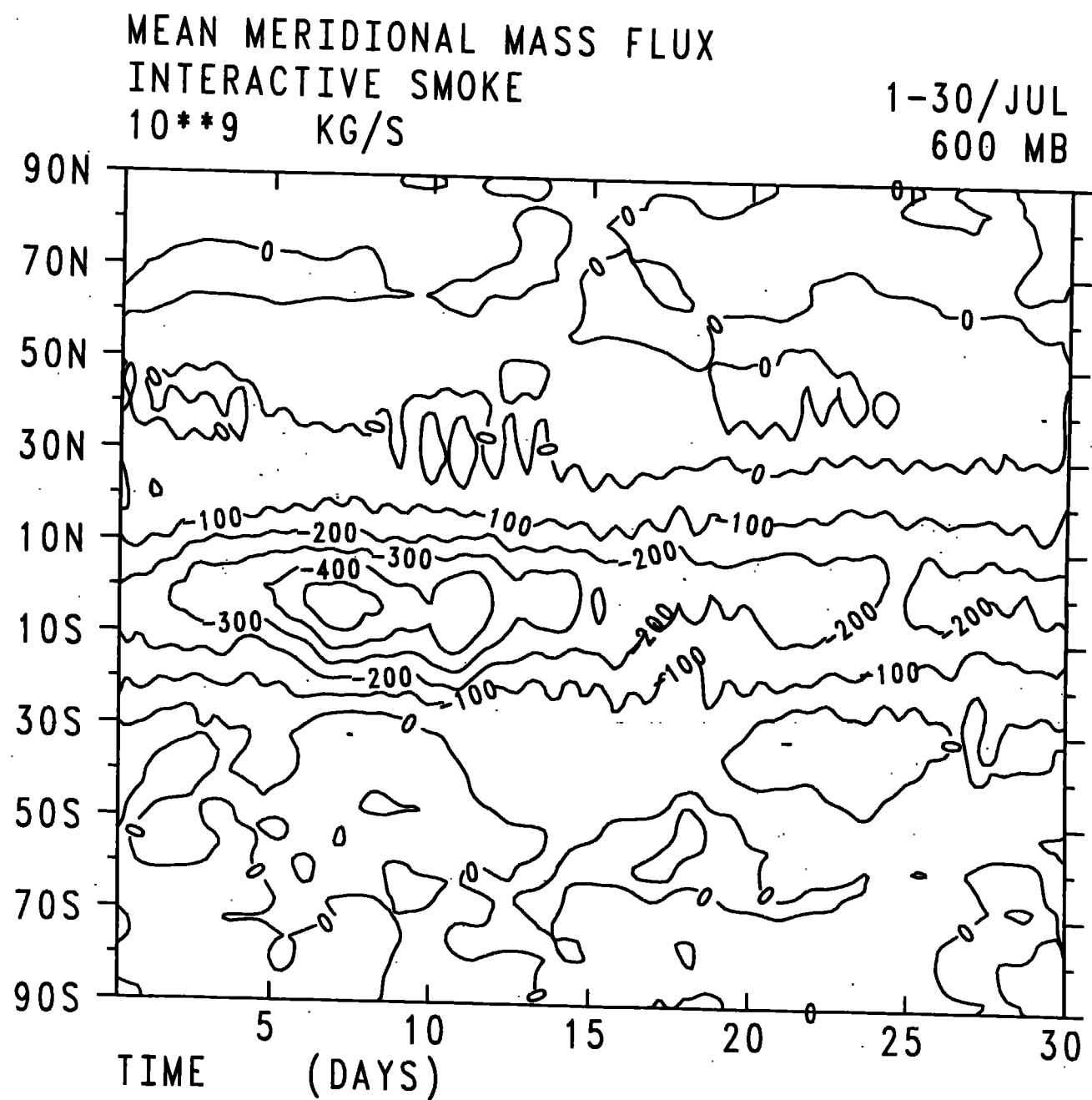


Figure 2. Mean meridional mass flux between 200 mb and 600 mb, integrated over all longitudes, for a 150 Tg interactive smoke simulation of July.

----- STANDARD DEVIATION

——— MEAN

CONTROL

TOTAL PRECIPITATION AT SURFACE

1-30/JUL

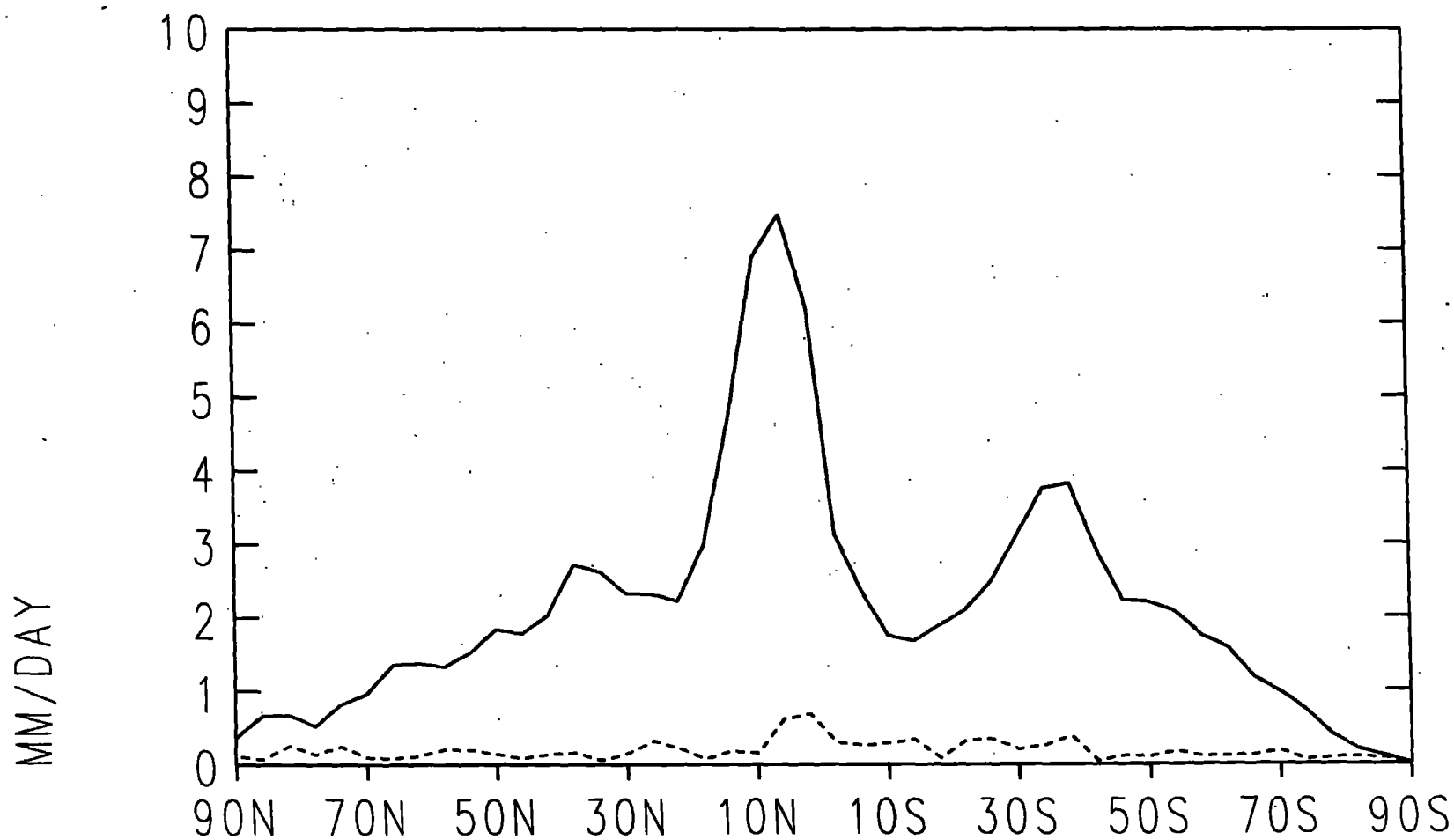


Figure 3. Time mean and standard deviation of 10-day means of zonal mean precipitation for a control (no smoke) July simulation.

----- CONVECTIVE PRECIPITATION AT SURFACE  
—— LARGE-SCALE PRECIPITATION AT SURFACE  
CONTROL

1-30/JUL

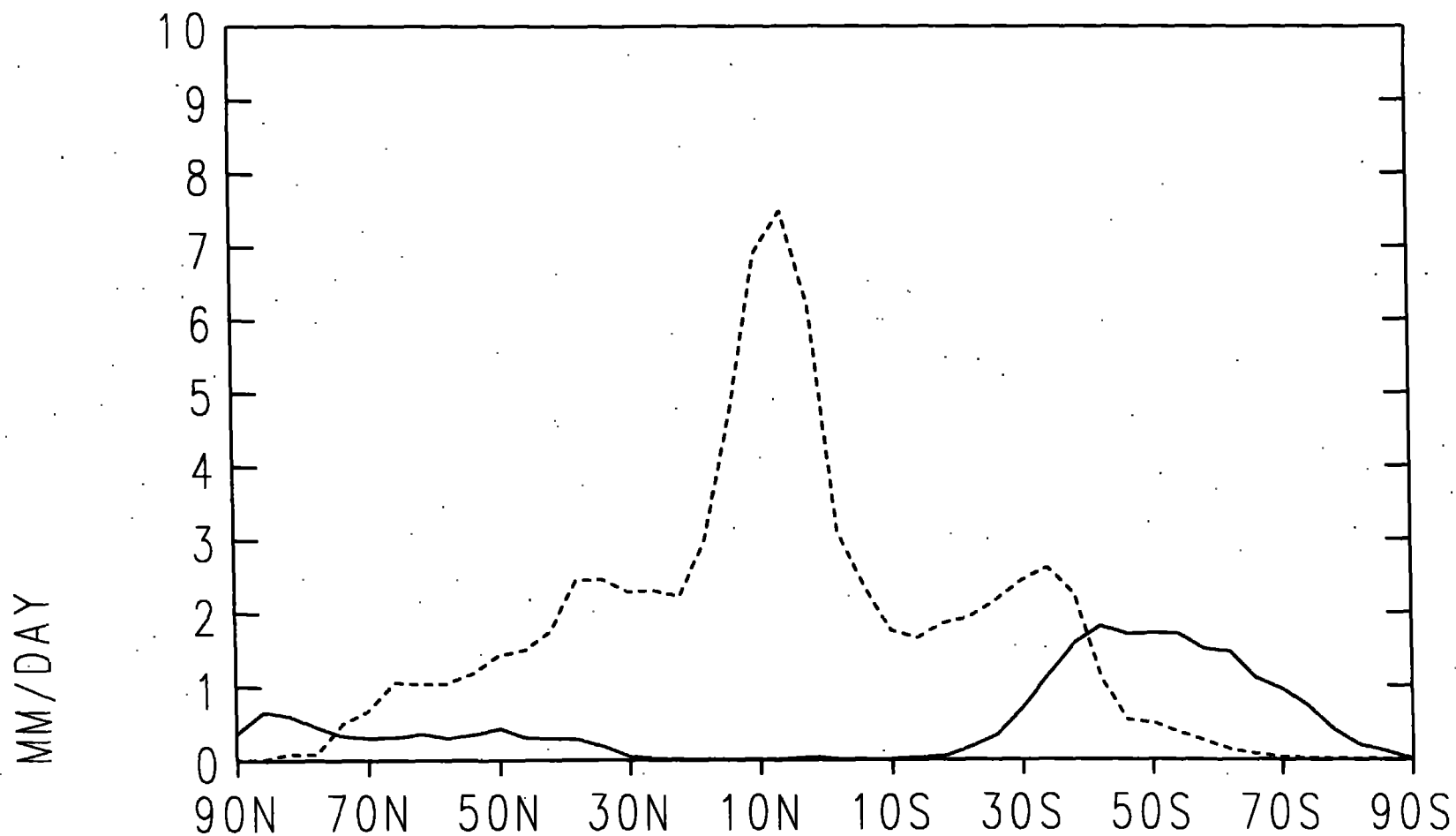


Figure 4. Time and zonal means of large-scale and convective forms of precipitation simulated for a control July climate.



--- SMOKE 21-30/JUL  
 ---- SMOKE 11-20/JUL  
 ..... SMOKE 1-10/JUL  
 ——— CONTROL 1-30/JUL  
 INTERACTIVE SMOKE  
 TOTAL PRECIPITATION AT SURFACE

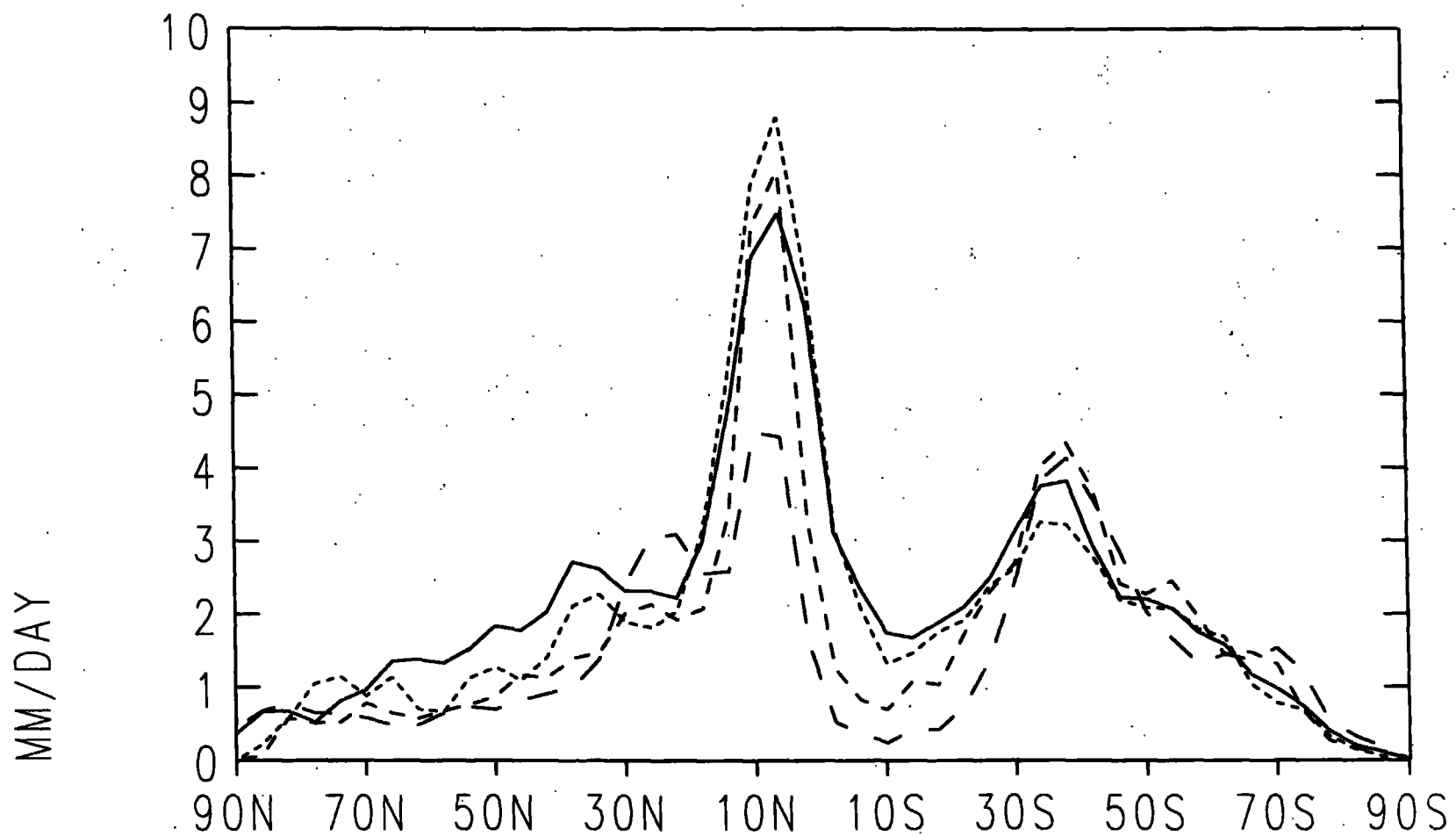


Figure 5. Zonal means of the total precipitation at the surface for a control July simulation and for days 1-10, 11-20, and 21-30 following a 150 Tg injection of smoke.

Figure 6. As for Fig. 5 but for convective precipitation only.

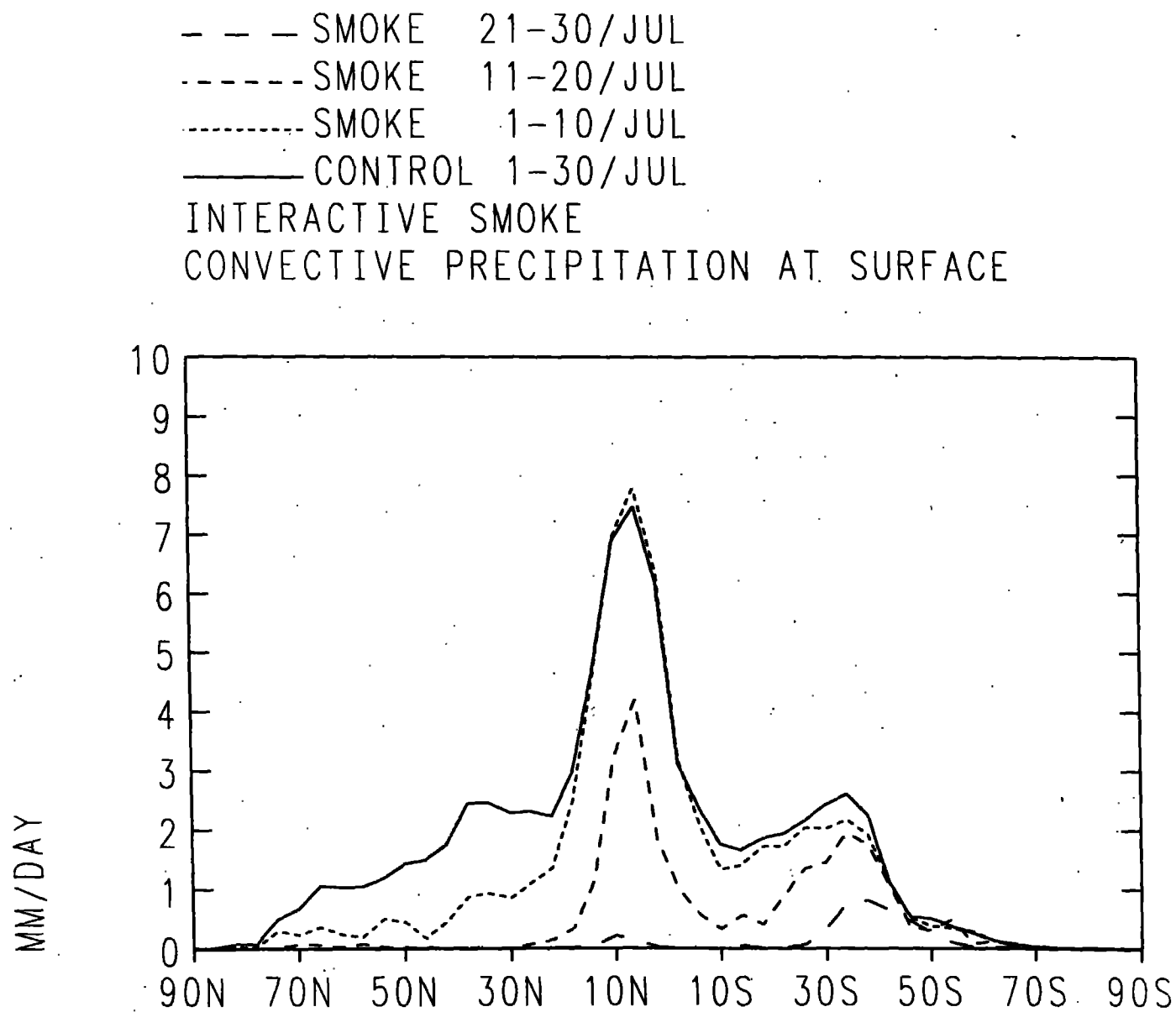


Figure 7. As for Fig. 5 but for large-scale precipitation only.

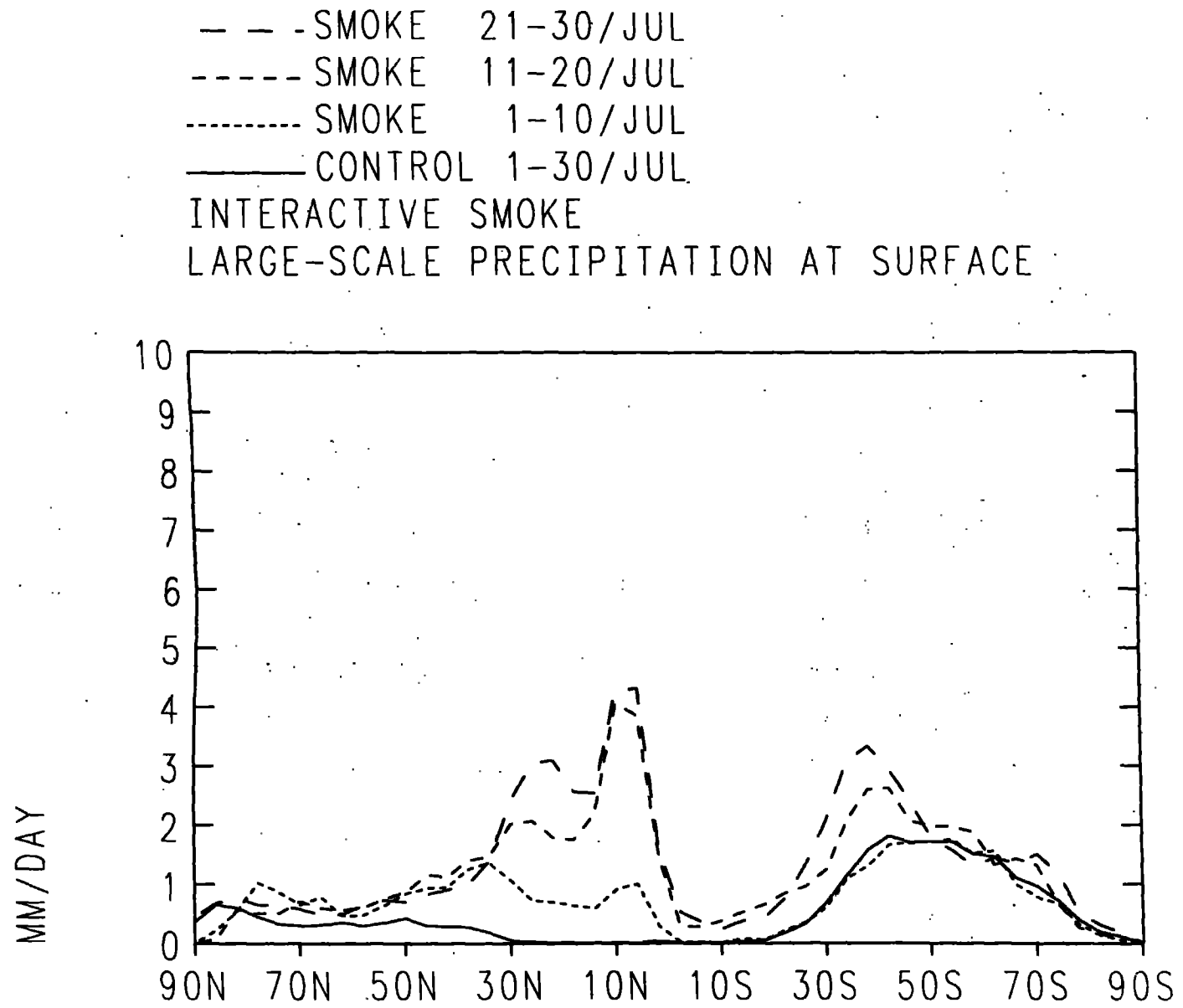


Figure 8. As for Fig. 5 but for ocean areas only. For latitudes with no ocean the land average is given.

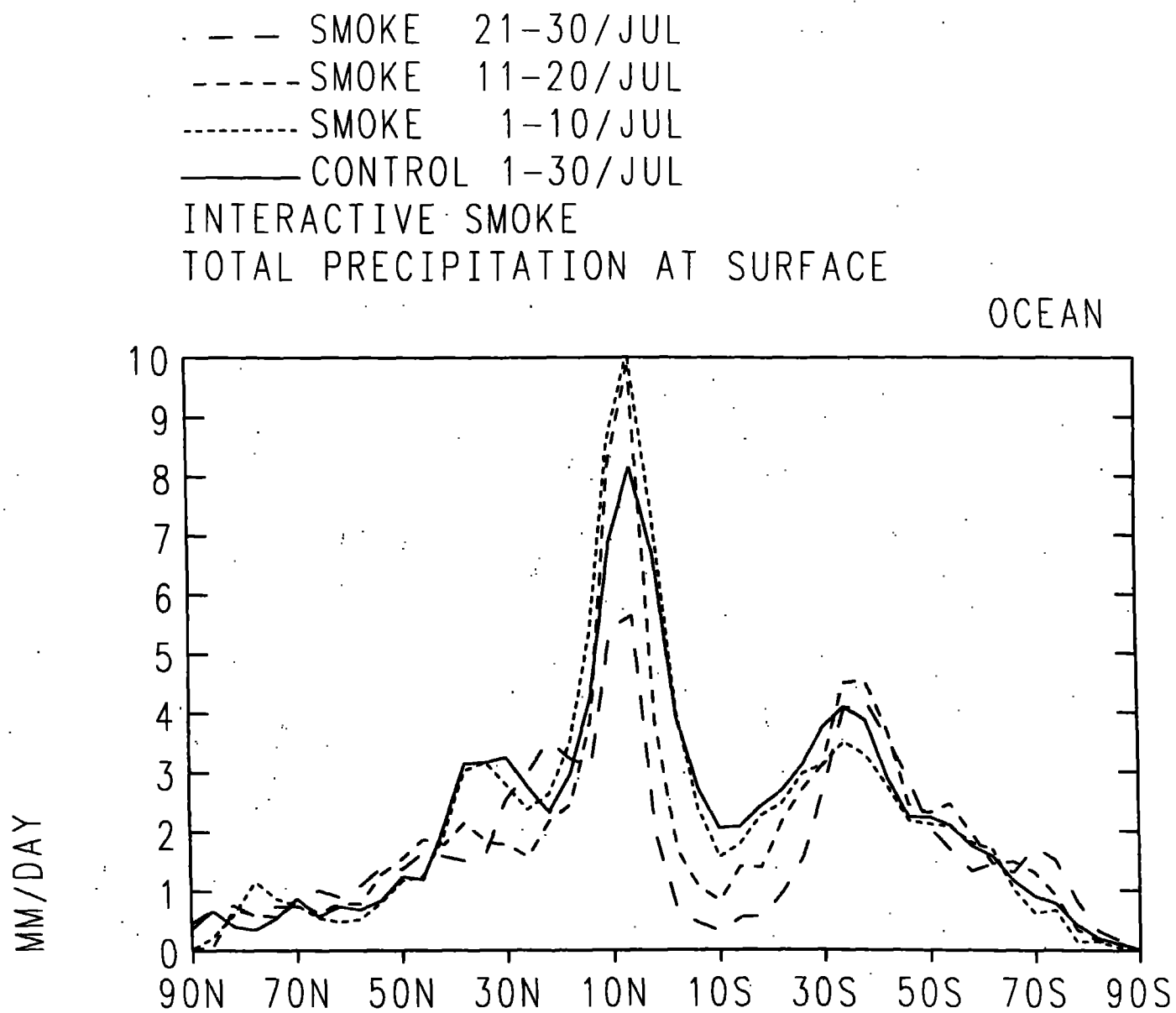


Figure. 9. As for Fig. 5 but for land areas only. For latitudes with no land the ocean average is given.

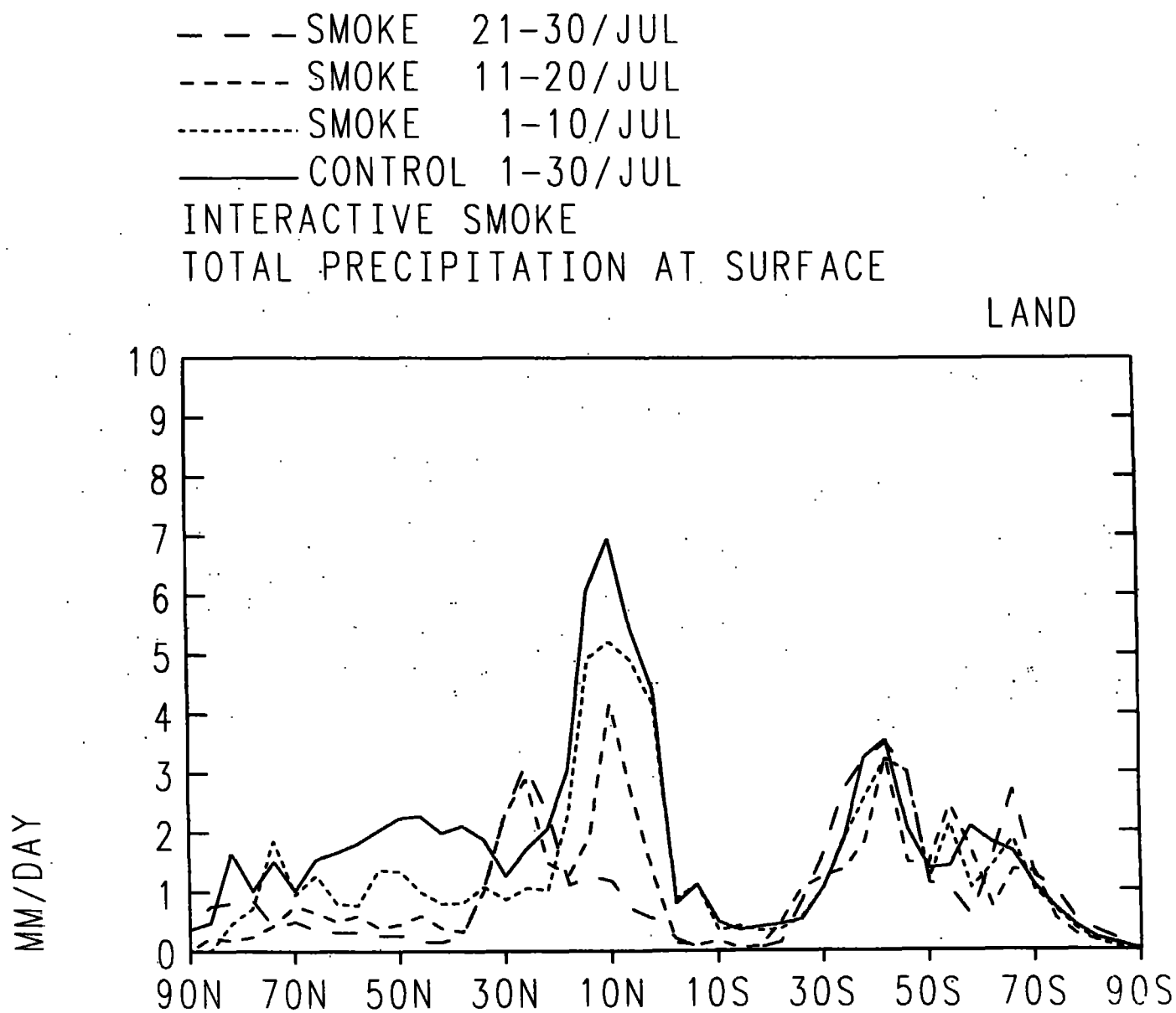


Figure 10. Change in land surface air temperature for days 1-10, 11-20, 21-30 following a 50 Tg smoke injection for July.

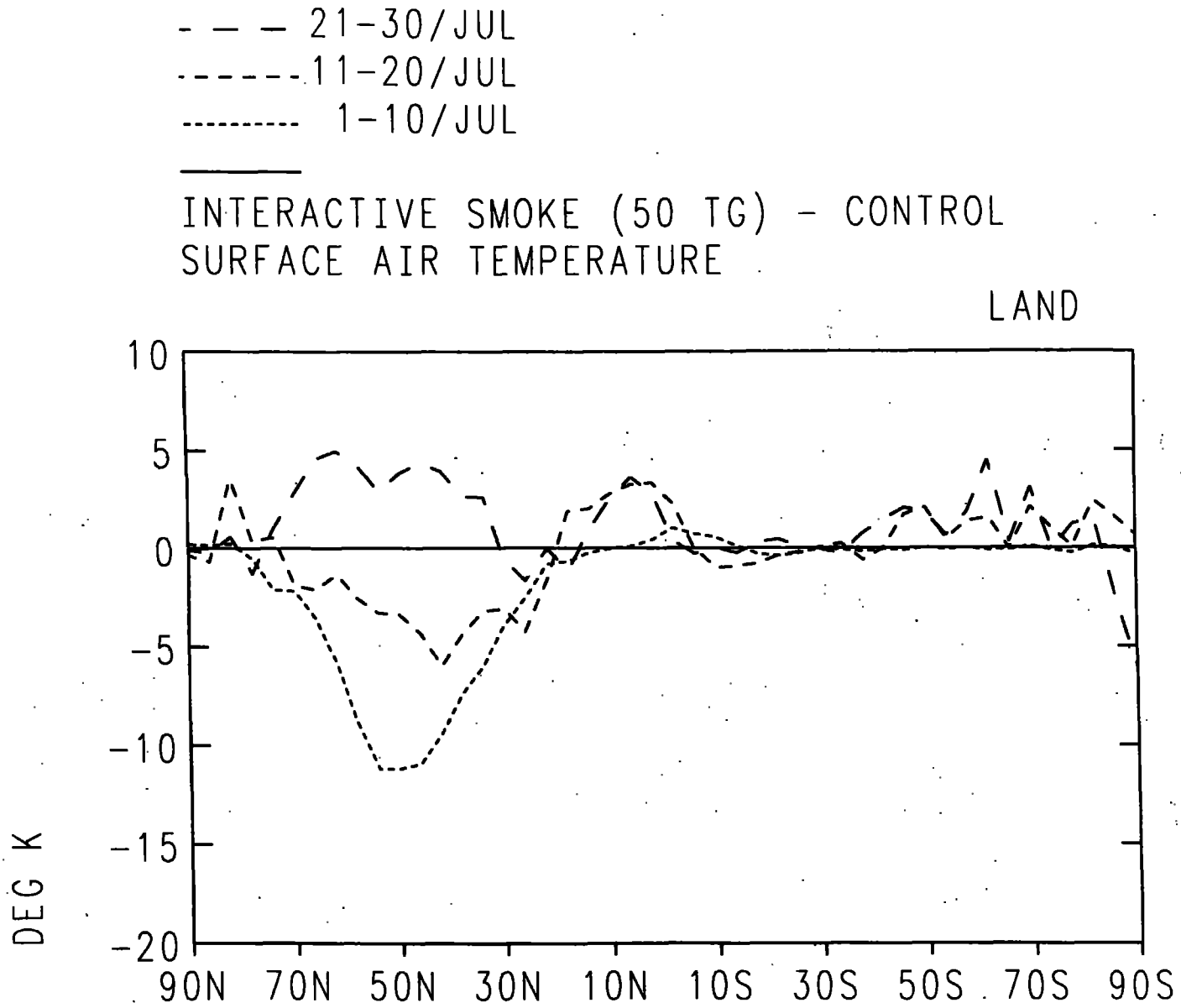


Figure 11. As in Fig. 5 but for land only and for a 50 Tg smoke injection.

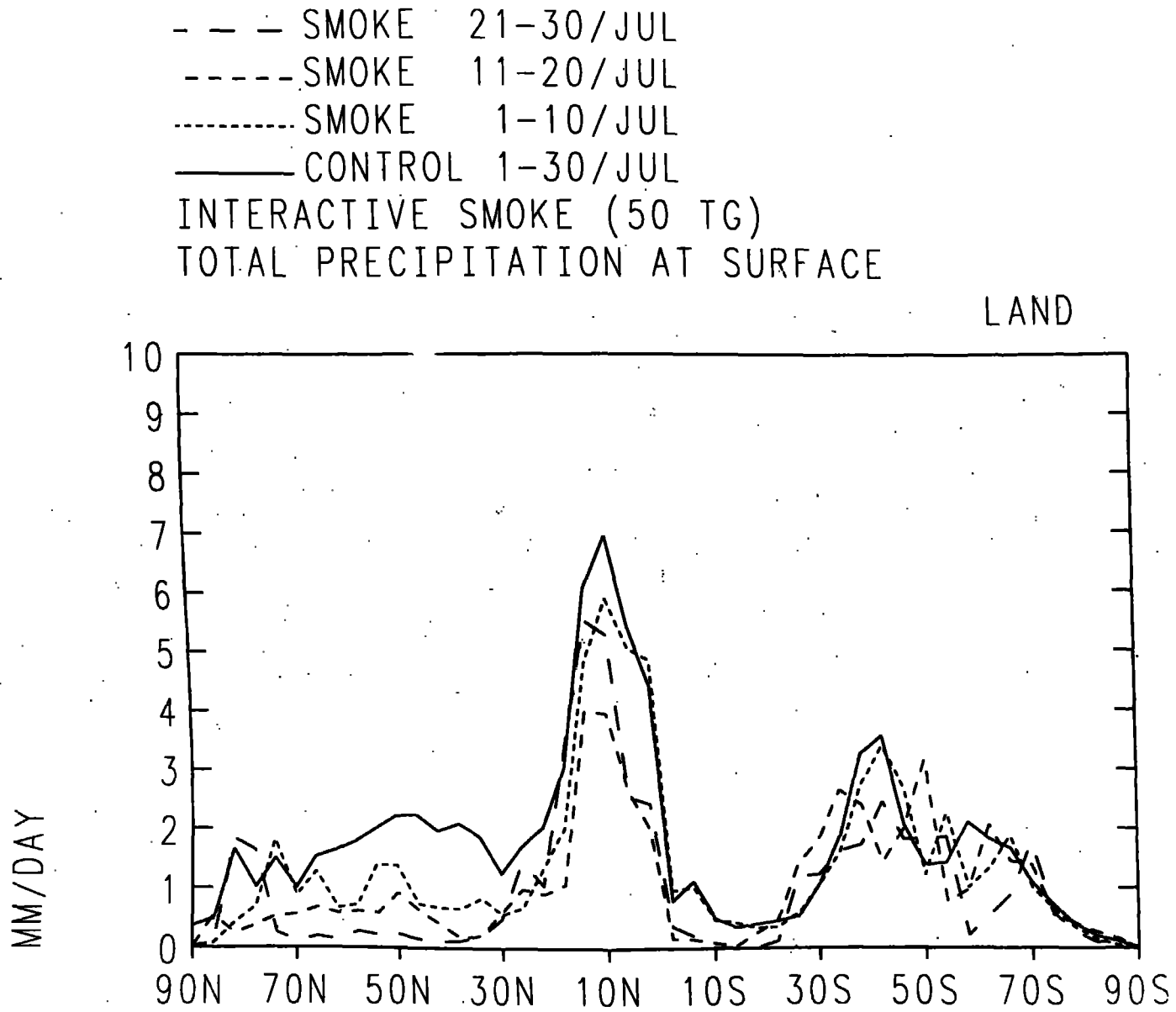


Figure 12. As in Fig. 5 but for the mid-level of the AGCM, which is at about 600 mb.

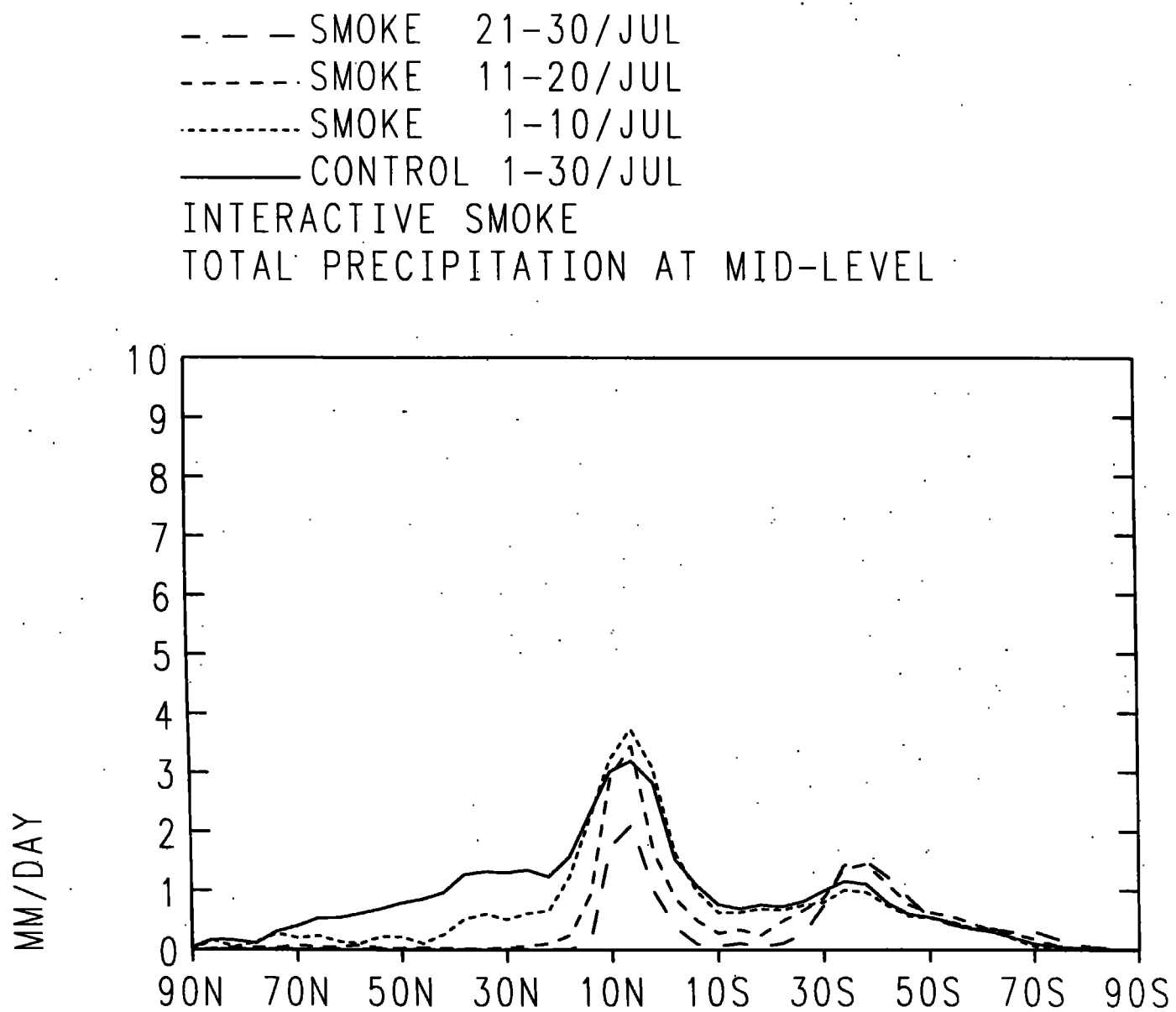
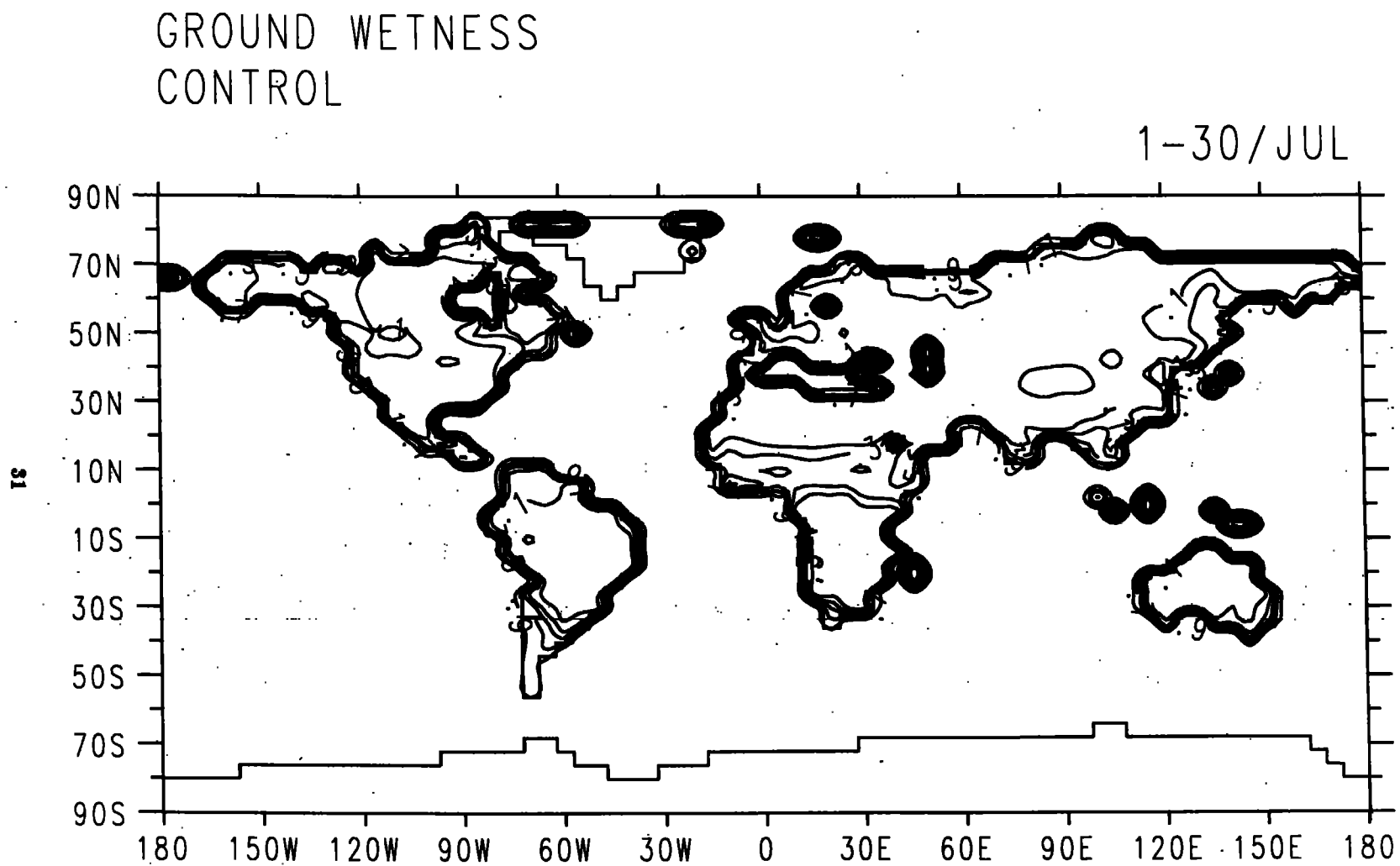




Figure 13. The simulated ground wetness (the ratio of the ground water content to the field capacity,  $15 \text{ g/cm}^2$ ) for the control July simulation. Contour levels are 0.1, 0.3, 0.5, 0.7 and 0.9.



GROUND WETNESS  
INTERACTIVE SMOKE

21-30/JUL

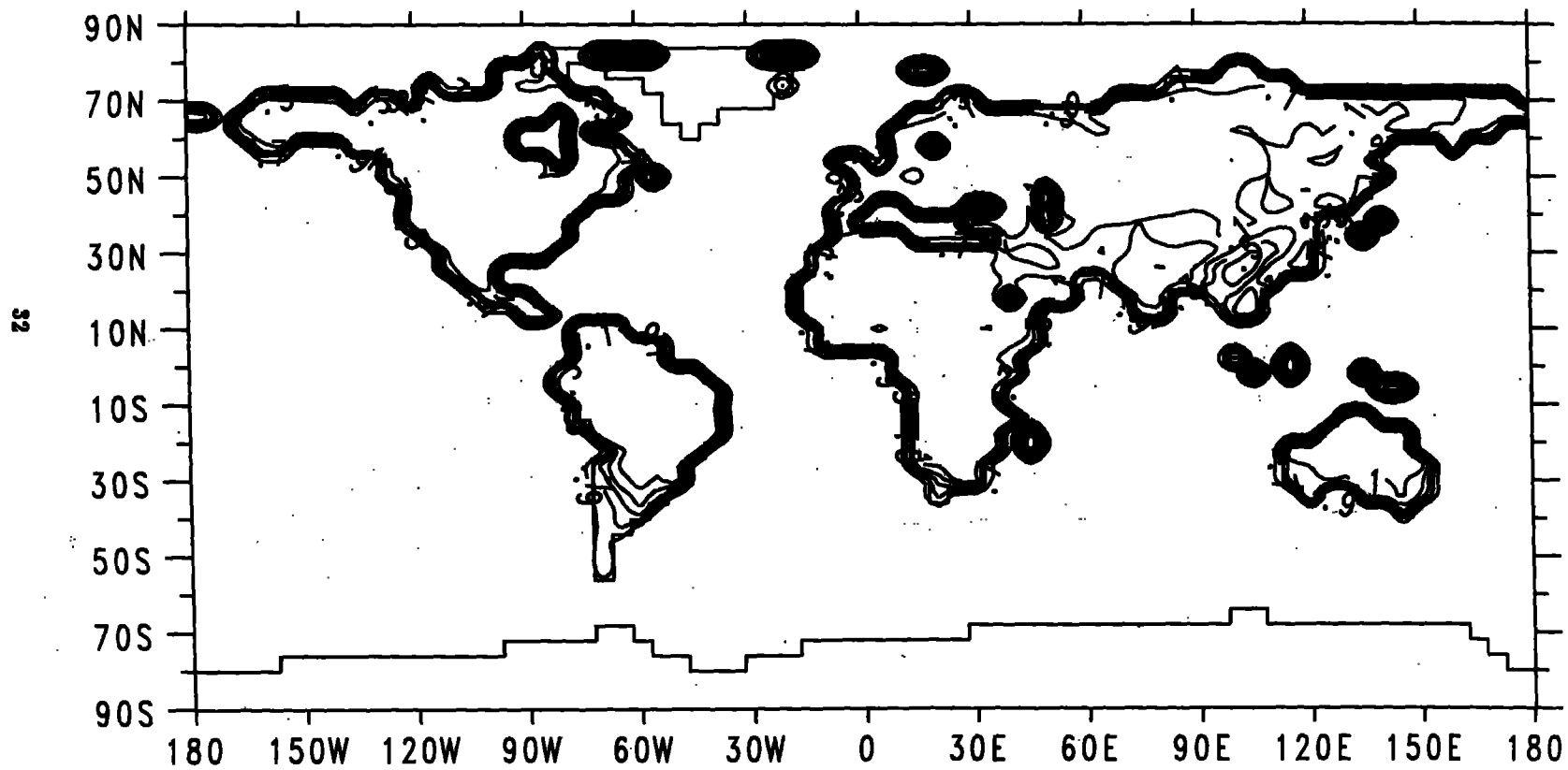


Figure 14. As in Fig. 13 but for days 21-30 following a 150 Tg smoke injection.

Figure 15. The change in surface air temperature for days 21-30 following a 150 Tg July smoke injection.

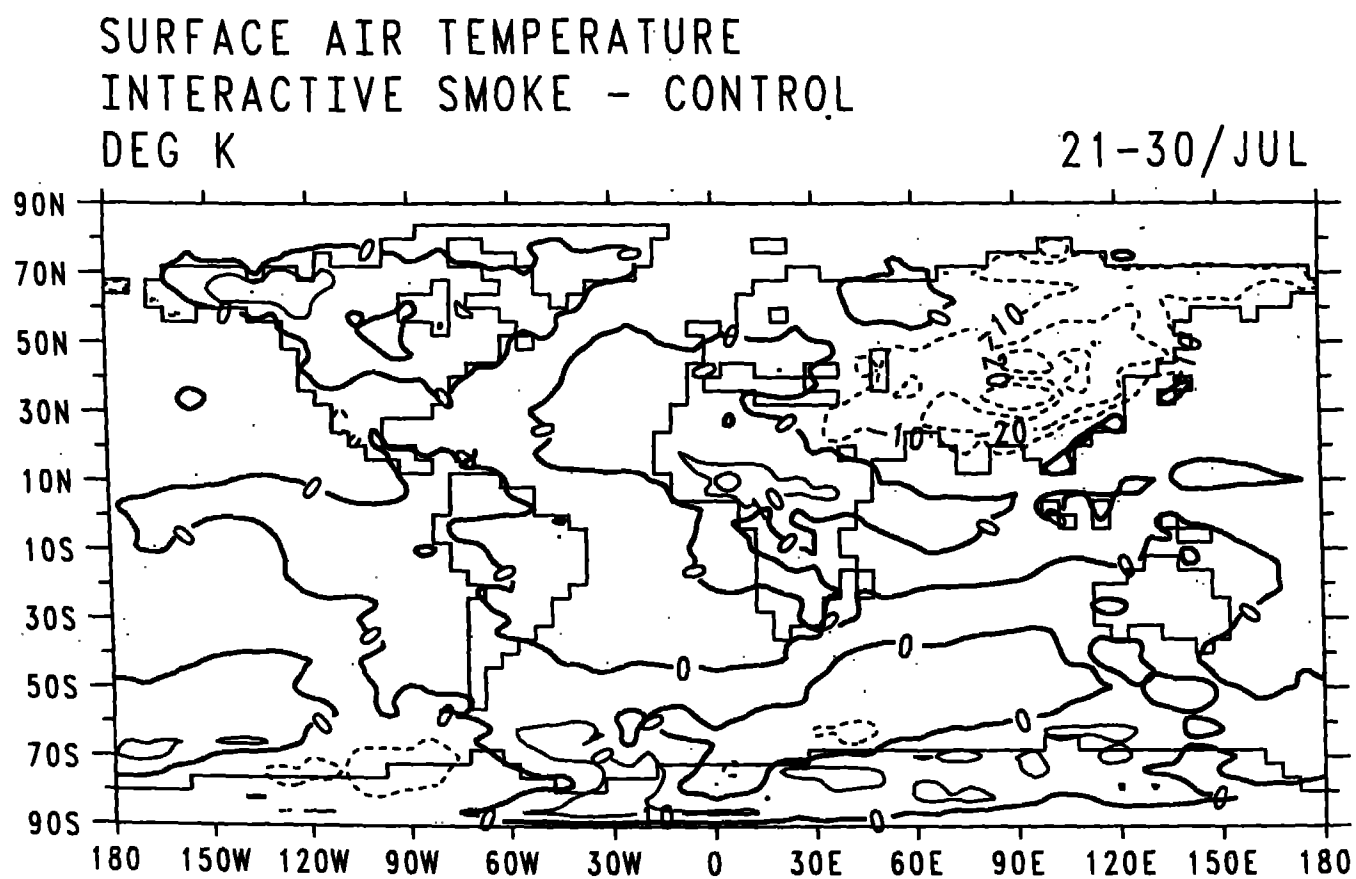


Figure 16. The globally integrated mass of large smoke particles for days 1-30 of a control (passive smoke) simulation and following a 150 Tg July injection of smoke.

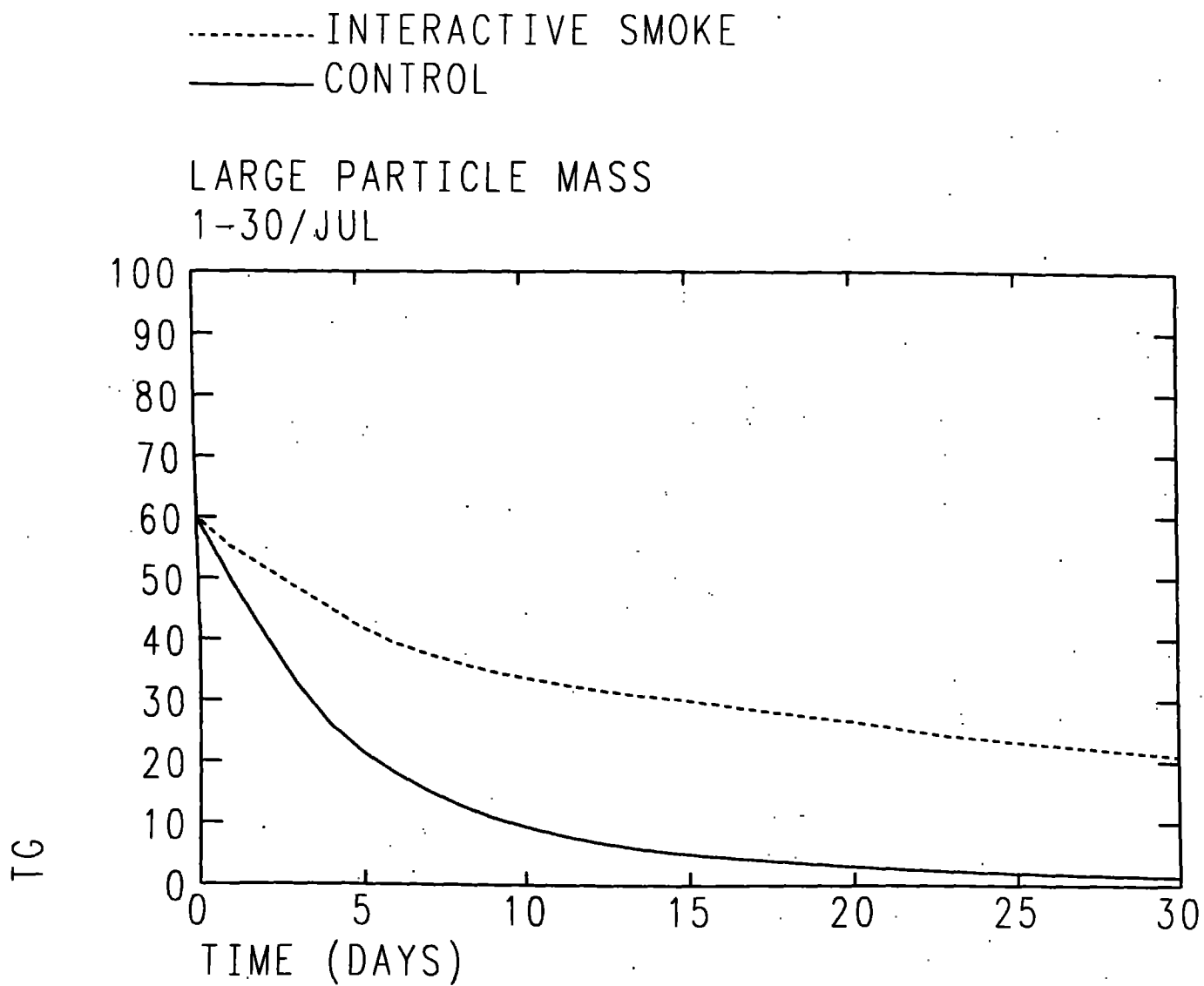


Figure 17. The lifetime of large smoke particles for control and 150 Tg interactive smoke simulations.

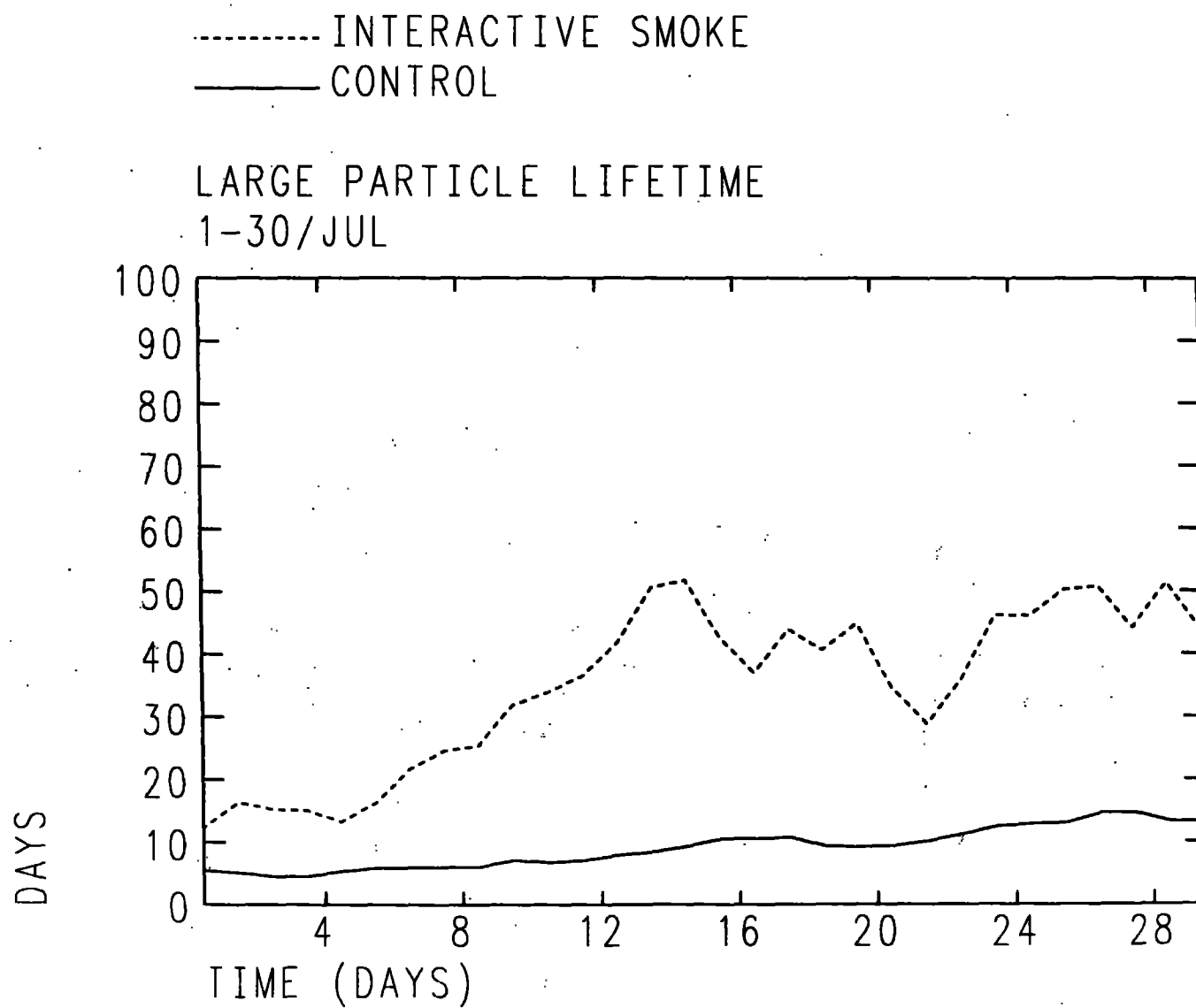
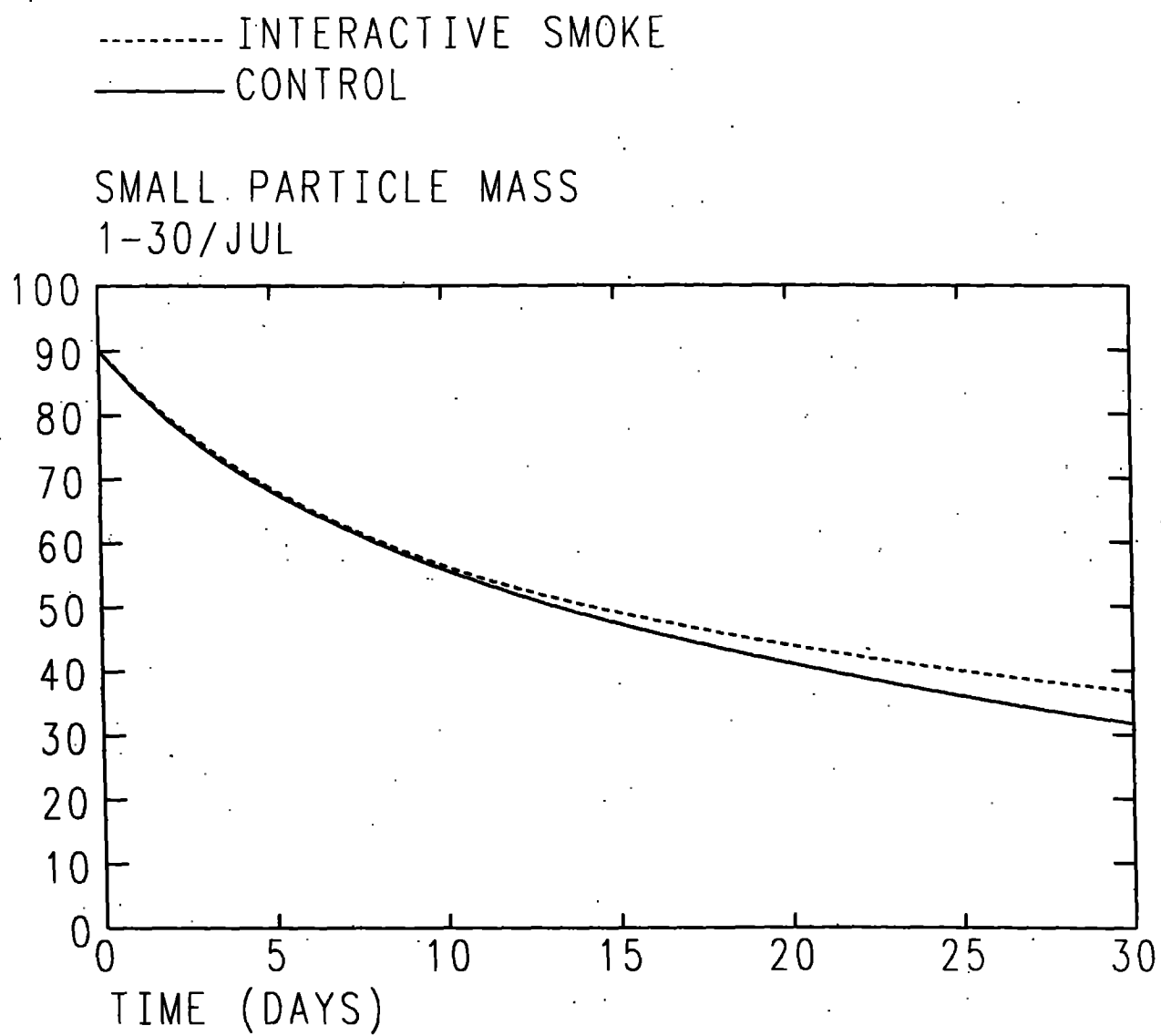


Figure 18. As in Fig. 16 but for small smoke particles.



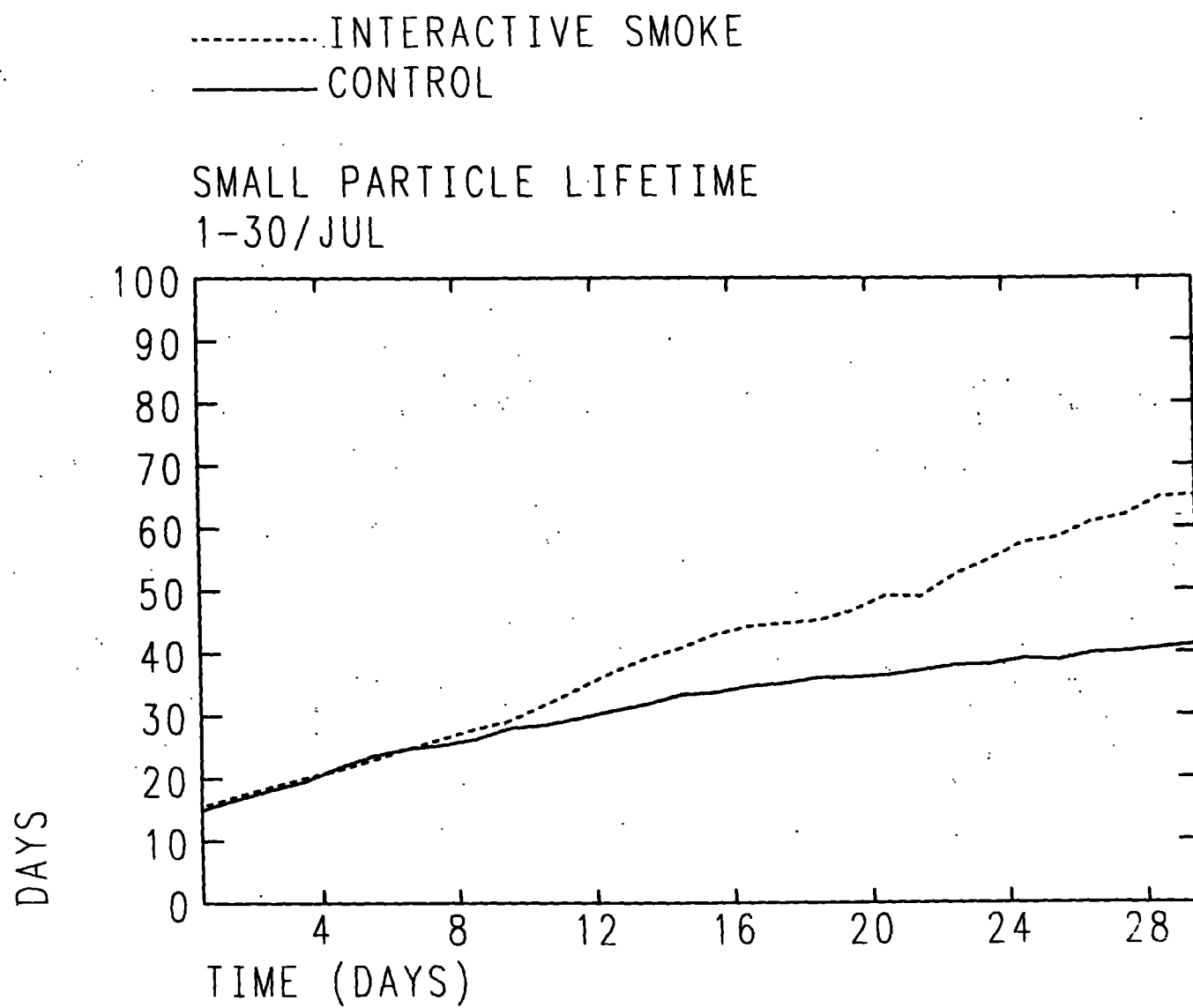


Figure 19. As in Fig. 17 but for small smoke particles.

Figure 20. As in Fig. 18 but for the total smoke mass.

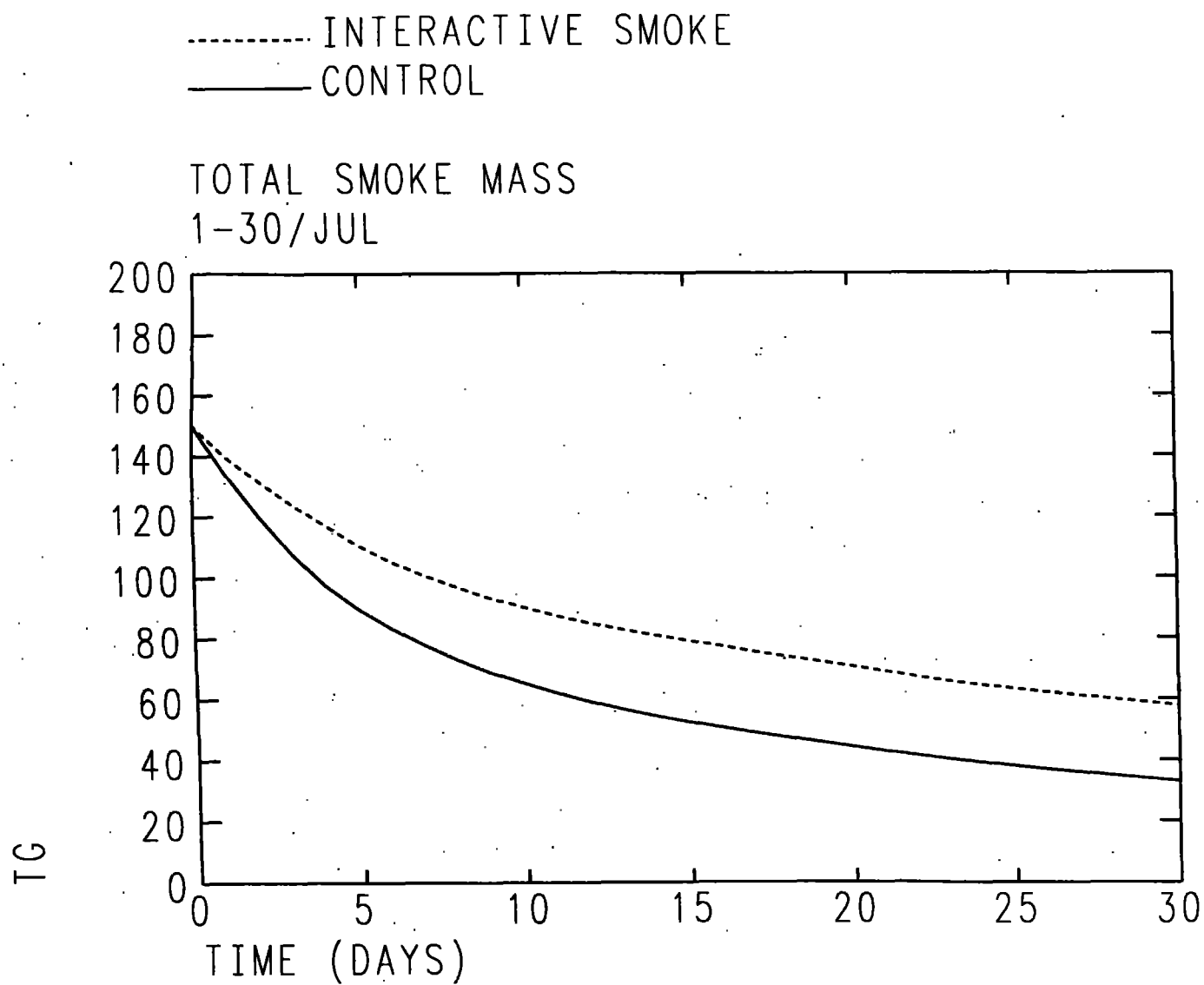
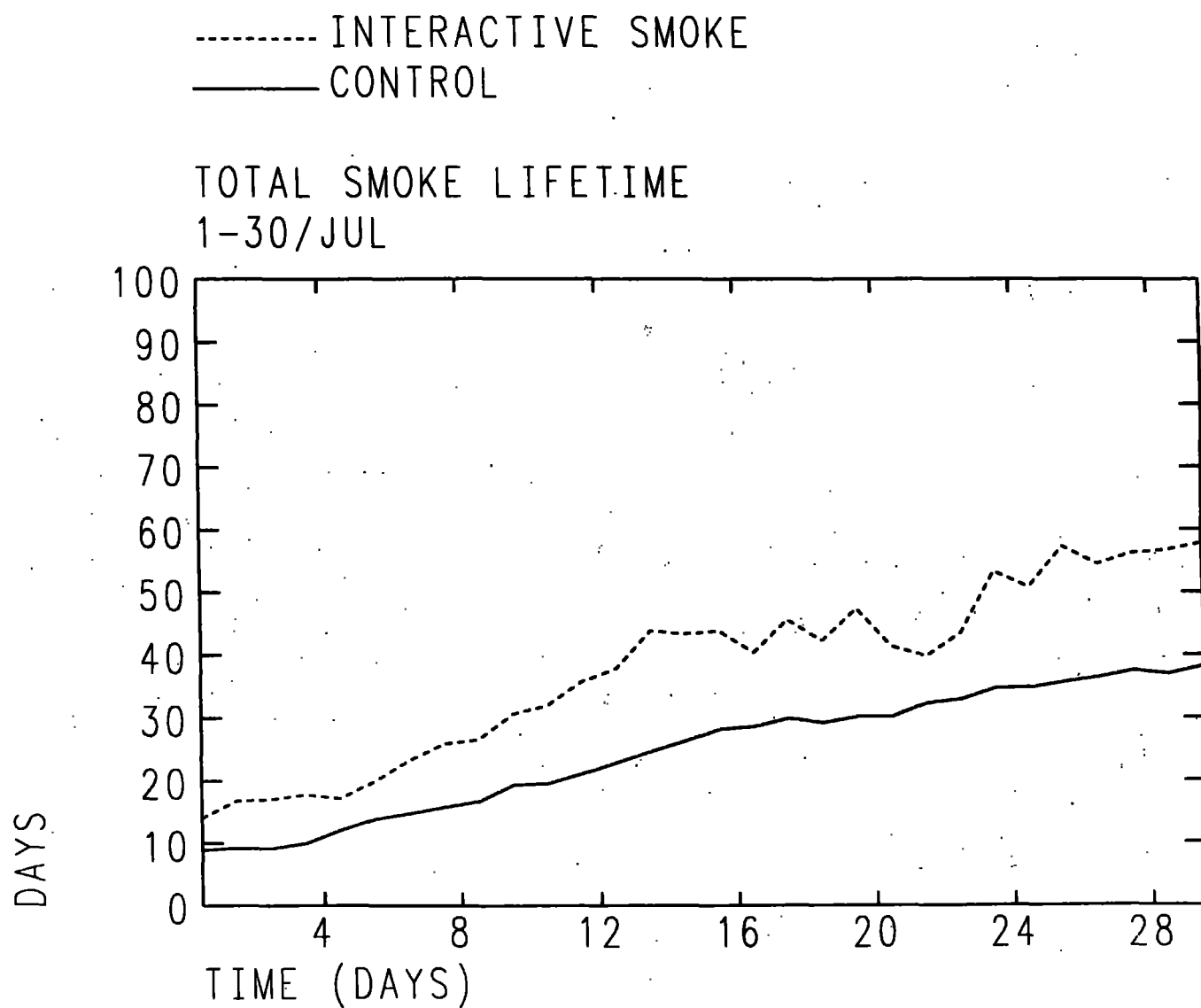




Figure 21. As in Fig. 19 but for the total smoke mass.



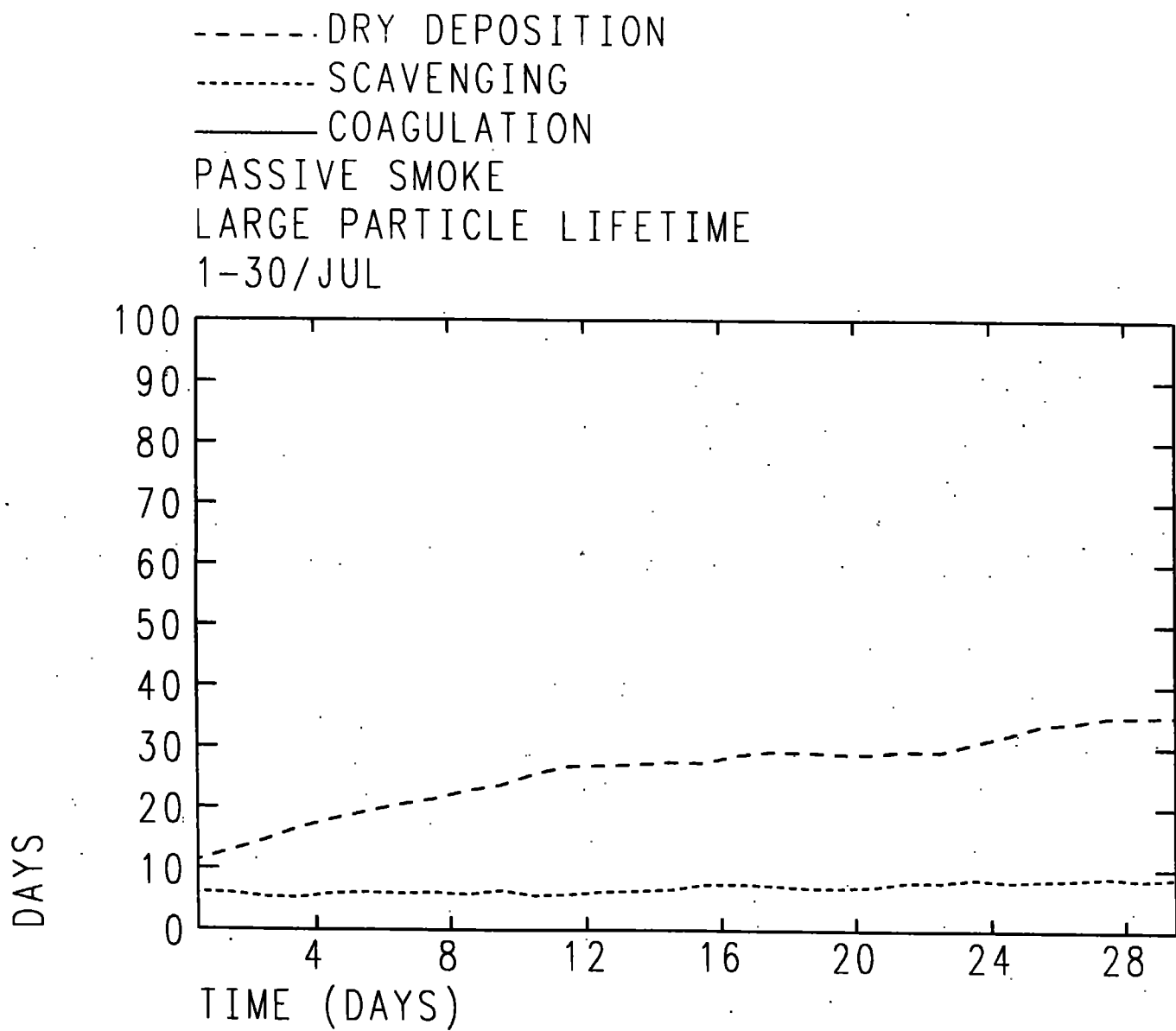


Figure 22. Lifetimes of large smoke particles for a control simulation, with removal by dry deposition, precipitation scavenging, and coagulation, individually. Note that, for large particles the coagulation lifetime is not defined.

Figure 23. As in Fig. 22 but for small smoke particles.

